Graphene oxide Composites: A versatile material used as protective layer, solid-state electrolyte, and gel electrolyte in metal batteries

Charlotte Maignan, Johan Alauzun, Emmanuel Flahaut, Laure Monconduit, Bruno Boury

Chemical Engineering Journal 485 (2024) 149616

Contents lists available at ScienceDirect

Chemical Engineering Journal

journal homepage: www.elsevier.com/locate/cej

Review

Graphene oxide Composites: A versatile material used as protective layer, solid-state electrolyte, and gel electrolyte in metal batteries

Charlotte Maignan [a,b], Johan G. Alauzun [a], Emmanuel Flahaut [b], Laure Monconduit [a], Bruno Boury [a,*]

[a] Institut Charles Gerhardt, Univ Montpellier, CNRS, ENSCM, 34095 Montpellier, France
[b] CIRIMAT, CNRS-INP-UPS, UMR N° 5085, Université Toulouse 3 Paul Sabatier, 118 Route de Narbonne, CEDEX 9, F-31062 Toulouse, France

A B S T R A C T

Obtaining a "good" electrolyte is one of the major obstacles to the development of new-generation batteries with metal anodes (Li, Na, etc.). Its stability, efficiency in conducting ions (Li^+, Na^+, …) quickly and in large numbers, environmental acceptable and ease of integration into industrial manufacturing processes are among the most important criteria determining the choice of materials to be used. In this review, we focus specifically on the different uses of GO's as part of the electrolyte in battery like M−metal (M = Li, Na, Zn…) or Vanadium redox flow battery as chemical modification of commercial separator; as component of new separator; as thin film and protective layers composite; and as filler in solid-state electrolyte composite with polymers and gel electrolyte. Analysis of the collected data allows to point out the efficiency and relevance of GO to improve stability, capacity and cyclability of the corresponding electrolyte in operating battery. The review also tries to identify the strengths and weaknesses of the different approaches in order to highlight the advantages and limitations of using GO in electrolyte production.

1. Introduction

1.1. General context

The electrolyte in storage systems such as batteries is today one of the main technological locks for the development of new generations of energy storage devices. However, the technologies currently on the market no longer have room for improvement, it is therefore necessary to switch to a new generation of batteries. To increase the energy density, the use of lithium metal as negative electrode would be the holy grail. Although the cathode will limit the full cell capacity, the possibility to use a very thin Li electrode will allow increasing the energy density of the battery as shown in Fig. 1. Furthermore, the safety of this battery will be enhanced using a polymer electrolyte, which presents higher mechanical properties than classical liquid organic electrolytes.

To develop high energy metal anode batteries such as (Li-S, Li-air or Li-O_2) three main issues have to be addressed: the formation of the so-called solid electrolyte interphase (SEI), the formation of metal dendrites and the ion shuttling.

To overcome these problems, various strategies can be proposed. One of them is the use of solid polymer electrolyte (SPE) pioneered by Armand *et al.* in 1979.[2,3] Using polymer electrolyte instead of flammable liquid organic solvents improves the battery safety and is effective in operating the Bluecar electrical vehicles (Bolloré Group, Hydro-Quebec patent) although with limited performance.

Within this context, GO has many advantages to design electrolyte material able to minimize both SEI, dendritic growth and ion shuttling. As briefly presented below, GO is produced by oxidation/exfoliation of graphite. Combining unique properties and easy to process, graphene oxide is currently considered as high potential material in many types of energy production or storage systems like fuel cells, batteries (Li-ion, Li-S or Li-O_2), redox flow batteries, capacitors (dielectric and supercapacitor).[4–8] Additionally, the attractivity of GO also relies on the fact that it gives access to reduced graphene oxide (rGO), another material that presents high potential for similar applications.

1.2. The electrode interface, dendrite growth issue and ion shuttling issues

In batteries, an electronic insulator and ionic conductive material must separate the electrodes,[9–12] the commercial technologies use solid, inert, insulating and porous "membranes", the separator, soaked in liquid electrolytes presenting high ionic conduction ($\sigma \sim 10^{-3} - 10^{-2}$ S cm^{-1}).

However, the different components of the electrolyte react at the surface of the electrode and produce the SEI, when the working potential lies outside their electrochemical window stability. The full understanding of the SEI is not achieved yet (53 reviews for "SEI" and "Battery" on Scifinder in 2022) but it results in the formation of a thin solid film of several nanometers polymeric organic–inorganic material

* Corresponding author.
E-mail address: bruno.boury@umontpellier.fr (B. Boury).

https://doi.org/10.1016/j.cej.2024.149616
Received 3 October 2023; Received in revised form 19 January 2024; Accepted 11 February 2024
Available online 21 February 2024

Nomenclature

↕	Thickness
DFT	Density Functional Theory
EC	Ethyl carbonate
ECl	Ethyl-cellulose
EDC	1-(3-Dimethylaminopropyl)-3-ethylcarbodiimidehydrochloride
EMC	Ethyl methyl carbonate
EC	Diethyl carbonate
DCC	N,N'-dicyclohexylcarbodiimide
DOL	1,3-dioxolane
DME	1,2-dimethoxyethane
DMC	Dimethyl carbonate
DMF	Dimethyl formamide
DMSO	Dimethyl sulphoxide
GF	Glass fiber
GEP	Gel polymer electrolyte
LiBOB	Lithium bis(oxalato)borate
$LiPF_6$	Lithium hexafluorophosphate
LiTFSI	Bistrifluoromethanesulfonimide lithium salt
LCO	Lithium Cobalt Oxide
LFP	Lithium Iron Phosphate
LMO	Lithium Manganese Oxide
LTO	Lithium Titanium Oxide
O_f	Oxygen-containing function
PAA	Poly(acrylic acid)
PAN	poly(acrylonitrile)
PC	Propylene carbonate
PDAAQ	poly(1,5-diaminoanthraquinone)
PEO	poly(ethyeneoxyde)
PEG	poly(ethyleneglycol)
PEGA	poly(ethylene glycol)diacrylate
PEGMA-EGDMA	poly(poly[ethyleneglycol)-methylether methacrylate)
PMMA	poly(methylmethacrylate)
PP	Poly(propylene)
PSS	Polystyrenesulfonate
P(SF-DOL)	poly(vinylsulfonyl fluoride-ran-2-vinyl-1,3-dioxolane)
PTC	poly(vinylidene fluoride-tri-fluoroethylenechlorofluoroethylene)
PTFE	Poly(tetrafluoroethylene)
PVA	poly(vinyl alcohol)
PVDF	poly(vinylidenedifluoride)
PVP	Poly(vinylpyrrolidone)
PVDF-HFP	poly(vinylidenedifluoride-hexafluoro propylene)
SEI	Solid Electrolyte Interface
SHE	Solid Hybrid electrolyte
SPE	Solid Polymer Electrolyte
SPEEK	poly(etheretherketone)
TCNQ	Tetracyanoquinodimethane
THF	Tetrahydrofuran 2,2,6,6-tetramethylpiperidine-1-oxyl
TPP-4DMAP	Triphenyl phosphite-4-dimethylaminopyridine

presenting inorganic-rich phases close to the electrode/SEI interface (Li_2CO_3, Li_2O and LiF for F-containing components), and organic-rich phases close to the electrolyte (Lithium ethylene glycol dicarbonate and ROLi, where R depends on the component of the electrolyte). An ideal electrolyte would master the formation of the SEI presenting the highest possible Li^+ transport without electron transport leading to further reduction of the electrolyte.

The second important issue that faces the development of M−metal battery is the dendrites and whiskers growth, corresponding to the formation of $Li_{(s)}$ multi-branching crystals with needle-like structure,[9] Lithium is particularly prone to this phenomenon responsible for short circuits leading to disastrous battery failure.

The dendrites initiation/formation/growth process results from de reduction of $Li^+_{(sol)}$ into Li that then form the deposit of $Li_{(s)}$ through very complex process, not yet fully understood.[13] Many parameters have been identified to play a major role, among which the concentration and diffusion of Li^+ cation in the electrolyte, the kinetics of reduction of Li^+ ions, the current density during the charge but also the mobility of the counter-anion, the mass transfer properties of the electrolyte and the surface heterogeneity of the initial $Li_{(s)}$ microstructure.[14] These parameters can lead to local depletion and heterogeneous concentration of chemical species,[15] aggregation on $Li_{(s)}$ of generated Li atoms according to a diffusion-controlled mechanism or their nucleation separately from the surface of $Li_{(s)}$ by a nucleation-controlled mechanism. Besides, the SEI composition, heterogeneity and growth, make the process even more complex and the different models are not yet able to take into account the dendritic growth.[9] Besides the use of GO, the most common strategies to overcome these issues are treatments of $Li_{(s)}$ by a sub-micron organic or hybrid film, additives in the liquid electrolyte for reacting with $Li_{(s)}$ surface, new separators, gel and solid-state electrolytes.

A third issue is the ion shuttling. All batteries, require a high and

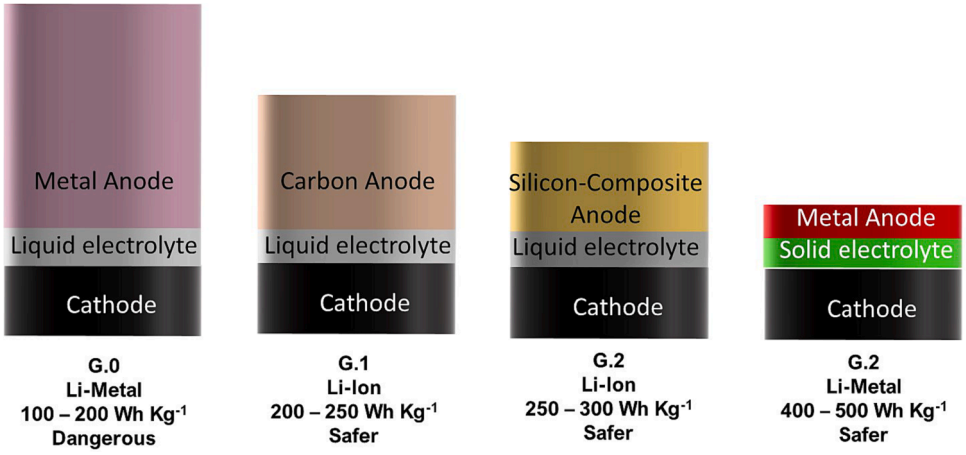

Fig. 1. Illustration of the different Li-batteries characteristic (capacity and safety); adapted from [1].

specific ion transport, either M^+ with M being a metal or H^+ in the case of Vanadium redox flow battery (VFB). In the case of Li-S, the use of inexpensive, abundant, and non-toxic sulphur as a cathode theoretically gives a specific capacity of *ca.* 1670 mA h g^{-1} with high theoretical specific energy of 2500 W h kg^{-1} or 2800 W h L^{-1}. However, the performances are severally limited due to the formation of soluble polysulphides (Li_2S_8, Li_2S_6, Li_2S_4, Li_2S_3, and Li_2S_2) that migrate to the anode and form a solid deposit after reduction. In VFB, the challenge is to inhibit the migration of VO_2^+ among others, while preserving the migration of H^+ and HSO_4^-/SO_4^{2-}. Similar problems are encountered in other types of aqueous flow battery systems.[16].

1.3. Aims & comprehensiveness of the review

Here, we excluded references mentioning graphene oxide in the formulation of the active material of the electrodes (example of recent reviews.[4,6,8,17–19]) applications of GO in fuel cells, or capacitors and supercapacitors. As illustrated in Fig. 2, we will only consider GO as part of the electrolytic domain as a coating, gel or solid electrolyte, alone or in a mixture, whatever its proportion and whatever the battery type.

2. What makes GO attractive for electrolyte & protective layers on separator & electrode

2.1. Synthesis & structure

The frequently used method to prepare GO is based on the work by Tour *et al.*[20] and following those of Hummers and Hoffeman in 1958.[21] This method by Tour *et al.* uses increased amounts of $KMnO_4$ and H_2SO_4:H_3PO_4 (9:1), helping to eliminate the release of toxic NO_x. GO became very popular with the beginning of the research on both graphene and related materials as a convenient alternative initial step to the direct physical exfoliation of graphite. Indeed, it has quickly been proposed as a convenient chemical exfoliation route of graphite to prepare GO, a precursor of reduced graphene oxide, initially claimed to be an equivalent of graphene.[22] The synthesis is simply performed in water with cheap and well-known reagents like permanganate (MnO_4^-), nitrate (NO_3^-), sulphuric acid (H_2SO_4), hydrogen peroxide (H_2O_2) acid and so on, specific reviews are dedicated to this.[23] Double oxidation of GO [24,25] or reoxidation of a reduced GO[26,27] are sometimes reported, generally aiming at increasing the level of O-containing (O_f) functions and limiting restacking.

The 2D structure of graphene oxide is the product of the oxidation of graphite layers according to the expected reactivity of carbon double

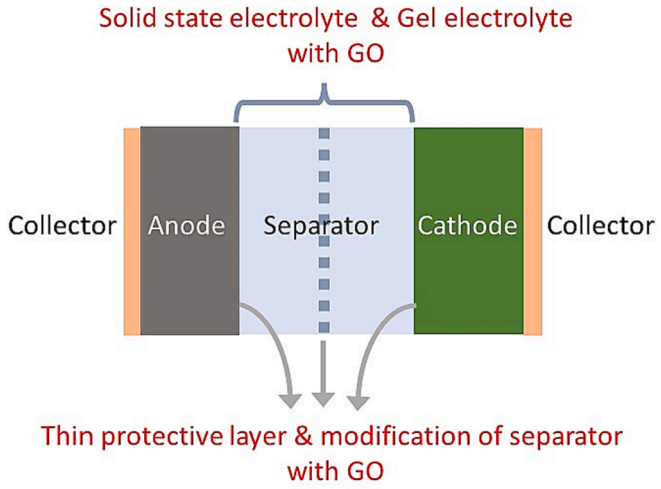

Fig. 2. Different uses of GO between the surface of anode to the surface of cathode in batteries.

bonds with strong oxidants. A precise and unique graphene oxide structure and/or composition do not exist, only different graphene oxides possessing similar properties and chemistry. The oxidation treatment produces O_f essentially alcohol, phenol, aldehyde, epoxide, quinone and carboxylic function. The ratio of these functions is highly dependent on the experimental procedure, an average C/O ratio being around 2. Fig. 3 summarized some properties brought by GO. A detailed description of the GO structure and functionality can be found elsewhere.[28,29] Layers can be several microns wide and present holes and an average 1 nm thickness for pristine graphene (≈0.34 nm).

GO aqueous suspensions (1 to 10 mg L^{-1}) are prepared mostly in basic conditions and some in acidic conditions. They can be processed by blading, spraying, dipping, 3D printing, etc.[30] To enhance the proportion of individual layers and avoid their stacking, sonication of GO suspensions is generally performed with classical ultrasound bath, but can induce massive fragmentation.[31] With increasing concentration, GO suspension behaves as discotic liquid crystals with very specific rheology and potential outcomes on their processing.[32–35] Such stacking of GO layers is a spontaneous process resulting from the aspect ratio of the GO layers and the hydrogen bonding between the OH functions. The structure is characterized in XRD analysis by a peak at $2\theta = 10.8^\circ$ corresponding to interlayer distance of ~ 8 Å (0 0 2) plane, the latter can vary from 5 to 9 Å, depending on the presence of intercalated molecules of water.[36].

The stacking of the GO layers results in high mechanical strength, poor hydrophilicity, and dramatically decreases the specific surface area to ~ 200 m^2 g^{-1} compared to the theoretical ~ 2500 m^2 g^{-1} (expected for individually separated layers).[38,39] Stacking allows preparing GO freestanding films and papers with several micron thickness by simple vacuum filtration on a membrane. Each of the submicron-size layer observed in these papers (Fig. 4) is made of hundreds of stacked individual GO layer. To avoid as much as possible the layers to stack, different strategies can be adopted to form "porous GO" such as aerogels, sponges or foams.[5,40] Freeze-drying is the simplest solution but has limited effect on stacking and leads to a twisted, randomly assembled and cross-linked sub-micron flakes with opened micro-to-macroporosity. When combined with ice-templating, freeze-drying leads to well-organised film of vertically aligned sub-micron size channels and few nanometers thick GO walls.[41] Fully separated layers are achievable by adsorption or grafting in solution of molecules, macromolecules, soft and hard templates like surfactants, polystyrene beads, metal nanoparticles or oxide nanoparticles.[42].

2.2. Properties

- *For filtration.* The report of an ultrafast migration of water through the nanochannels of stacked GO,[43] has opened the ways to many different approaches to nano and molecular separation.[44–46] Such migration of water is generally described as a cooperative process occurring within nanochannels of the interlayers. Their size determines the selectivity of the membrane: the solvated species of larger size are selectively blocked at the entrance of the nanochannels, the solvated species with smaller size being able to enter and migrate through this space. Defects and holes in the GO structure, which account for an average of 2 % of the total surface area, cannot explain the high permeability of aqueous solutions.[47] Besides, other phenomena operate in this process, one being coordination of O_f function with transition metal cations while alkali and alkaline-earth ions tend to interact with non-oxidized regions by cation/π interactions. Additionally, the negative charge of phenolate and carboxylate groups can limit entrance to anions similarly to what is observed in the Gibbs-Donnan effect.[48].

These phenomena explain why GO was chosen in electrolyte material to allow the migration of metal ions and prevent that of other species like sulphides. In their seminal work, Zhang *et al.* assumed that not only GO can accommodate volume expansion of the S-cathode, its functional

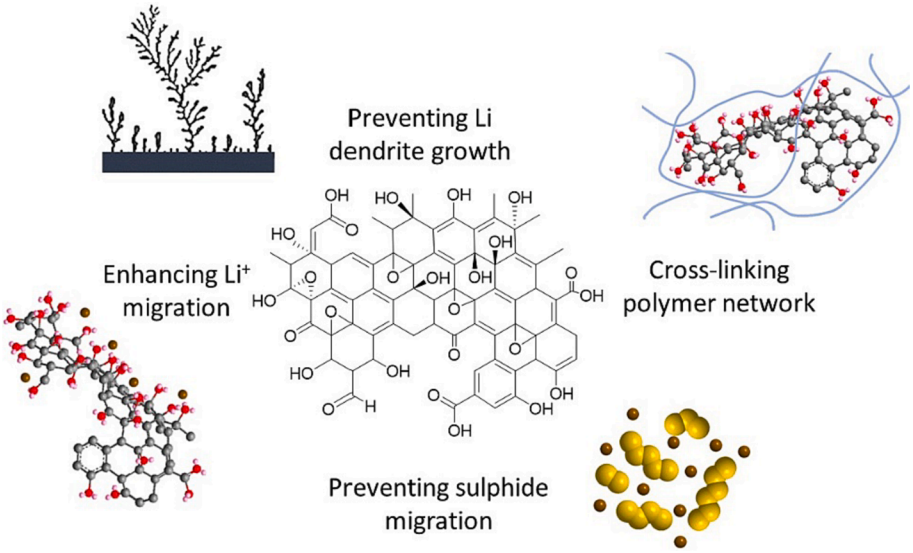

Fig. 3. Representation of the GO structure and of the four main phenomena properties.

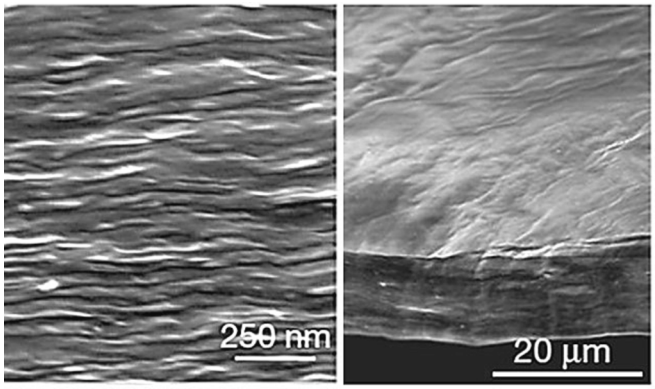

Fig. 4. High-resolution SEM side-view images of 10-mm-thick sample of a GO paper; permission from ref.[37] copyright (2007).

groups "both epoxy and hydroxyl groups of GO can enhance the bonding of S to the C-C bonds due to the induced ripples by the functional groups".[49] Additionally, non-porous GO films efficiency to block the sulphides originates from both their repulsion with the negatively charged GO nanolayer and their size larger than the interlayer space. Another example of this has been reported for vanadium redox flow battery,[50] a molecular sieving operating efficiently by blocking the transport of oxovanadium ions throughout GO, while allowing the transport of H^+.

- *Thermal stability.* Spectroscopic analyses evidence that after loss of residual water, thermal reduction of GO starts around 180 °C, a temperature much higher than the working batteries considered today.[51,52] However, this may strongly depend on the experimental conditions such as pressure in particular but also the nature of the atmosphere. A fast-heating rate can potentially lead to explosive thermal decomposition),[53] typically between 180 and 200 °C. Once this exothermic decomposition step is completed, thermal reduction continues with increasing temperature but at a slower pace and full thermal reduction is only reached at very high temperature. Besides, GO improves in some cases the thermal stability of the polymer with which it is associated but this occurs at temperatures higher than the reduction of GO (ca > 200 °C) and questions the state of GO in these conditions.

- *Electrochemical stability.* GO is known to react electrochemically, its electro-reduction is an alternative to chemical or thermal reduction to prepare rGO.[54,55] Different studies have established that O_f functions start to reduce at *ca.* −1 V (vs Ag/AgCl) on various substrates and at different pH.[55–5758,59] The reduction of GO to rGO by contact with Li anode upon cycling[60] or by contact with Li is also known.[61,62] Obviously, the formation of H_2 is expected according to standard potential of reaction of alcohol function with lithium, but if rGO is formed this implies the reduction of the O-bounded carbon atoms of GO for example with formation of lithium hydroxide or oxide. Such reaction between GO (0.6 V *versus* SHE) and Li (-3.04 V *versus* SHE) according to eq. (1) is assumed to produce an"etching" of the growing dendrite and represents an additional tool to prevent this issue.[63,64]

$$2\,Li + GO \rightarrow Li_2O + rGO \quad (1)$$

The electro-reduction of GO is widely studied, but the electro-oxidation is rarely described although it is important in the perspective of high voltage batteries. Chemical oxidation of GO is possible, recently it was demonstrated that it is an interesting approach of the synthesis of MnO_2, GO also acting as a sacrificial template.[65] Besides, in a comparative study between graphene oxide and reduced graphene oxide,[66] Xu *et al.* ascribed the higher capacitance of GO over rGO to the pseudo-capacitance of GO resulting from electrochemical oxidation according to eq. (2). Note that, for high potential Li-metal batteries, the ideal stability range is 0 to 5 V *versus* Li/Li^+.[67]

$$> CH - OH \rightarrow \; > C = O + 2H^+ + 2e^- \quad (2)$$

- *Conductivity.* The electronic conductivity of GO ($3.94\ 10^{-6}$ S m^{-1}) is much lower than the one of graphene (498 S m^{-1}) but it is reported that pressing each of them with carbon black results in much closer values, respectively 87.7 S m^{-1} and 136.6 S m^{-1}, unfortunately pressure value is not reported by the authors.[66]

Differently, the proton conductivities of GO is relatively high, Hayami *et al.* reported a $\sigma \sim 10^{-2}$ S cm^{-1} at 95 % relative humidity above 340 K, a value that approaches that of commercial proton conductors such as Nafion™.[68] H^+ conductivity varies with the presence of epoxy functions,[69,70] and also with the thickness of the GO layer. The proton conductivity increases very quickly for thickness between < 60 nm ($\sigma = 1\ 10^{-6}$S cm^{-1}) and 200 nm ($\sigma = 4\ 10^{-4}$S cm^{-1}) and then decreases slightly for thickness between 200 nm and 1 µm.[69] Epoxide groups are assumed to be the major contributors to the efficient in the proton transport process. Consequently, GO is considered as an important potential candidate in the development of ion exchange membranes for fuel cells and other batteries based on H^+ migration, for example lead

battery.[71].

For Li-ion or Li-metal battery, the targeted ionic conductivity is between 10^{-3} and 10^{-2} S cm^{-1}, close to that of usual liquid electrolyte (10^{-1} to 10^{-3} S cm^{-1}). Publications rarely mention the ionic conductivity of the GO alone that is prepared and used, a situation merely understandable when considering the variability of GO in composition, size, aggregation degree, etc. Through more than 200 references, we have identified only two values that differ by a factor of 1000: $\sigma = \sim 6 \times 10^{-8}$ S cm^{-1} [72] and $\sigma = 7 \times 10^{-5}$ S cm^{-1}.[73] In the latter, a study on GO/PEO composites, Li *et al.* concluded with: "The results suggest that GO nanoplatelets are neither electrical nor ionic conductive and therefore can be used as a passive filler in the nanocomposite electrolyte".[74].

- *t_{Li} + transference number.* The Li^+ transference number t_{Li+} can be defined as the ratio of Li^+ mobility to the total ionic mobility as given in relation (1) where D is the self-diffusion coefficient of Li^+ and its counter anion A^-.

$$t_{Li^+} = \frac{D_{Li^+}}{(D_{Li^+} + D_{A^-})} \qquad \text{relation 1}$$

Recent studies demonstrate that beside ionic conductivity, t_{Li} + is determining for battery performance like charge–discharge capability [75] and suppression of the lithium dendrite growth (presented below).[76] t_{Li} + can be lower than 0.5, generally between 0.2 and 0.4, for conventional liquid electrolyte, an ideal t_{Li} + would be equal to 1, as in some of the solid state ceramic electrolytes. To the best of our knowledge, a t_{Li} + value for GO has never been reported.

- *Dendrite Growth.* As we will observe in the references below, the presence of GO associated with separator and with polymer in SPE frequently decreases the growth of lithium dendrites. Shahbazian-Yassar *et al.*,[77] in the case of a Li plating on a Cu collector covered by a nanofilm of GO/PVDF (↕ 0.2 μm, ≈50 μg cm^{-2}) ascribed the effect of GO layer to its lithiophilic nature which may be explained by both the high defects density and the layers stacking, able to "buffer" the migration of Li^+ cation; see Fig. 5 for illustration of the phenomenon. This tends to standardize, homogeneously and randomly distribute cations migration.

In addition, the mechanical properties of GO help to limit the "tip effect" and thus the dendrite formation. Similarly, for a mesoporous GO-polypyrrole coating on a copper collector, Wu *et al.* attributed to GO a nano-sieving effect that could "sufficiently slow down the shuttling speed of Li ions between electrodes, and reduce the Li dendrite growth rate, especially at high current densities".[78].

However, another effect of GO has been reported in the case of the Zn/MnO_2 battery, where the inhibition of Zn dendrites is also observed. For Zhang *et al.*, GO led to a homogeneous nucleation and deposition of Zn, but also to a preferential growth orientation. Indeed, the presence of GO in contact with Zn leads to the dominance of the (0 0 2) plane of Zn and the absence of the (1 0 1) plane.[79].

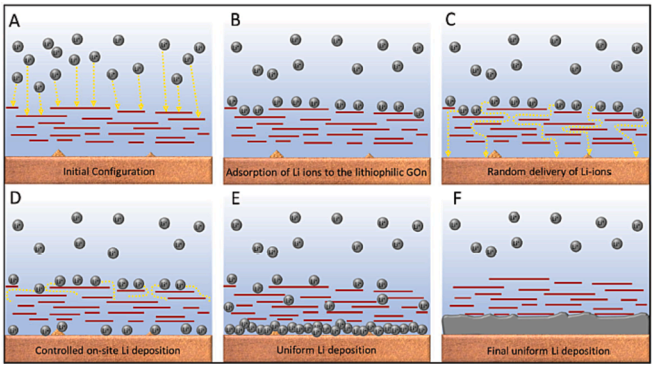

Fig. 5. Schematic view of Li deposition mechanism in case of GO-modified samples. A–F) adsorption of Li-ions to the lithiophilic GO coating and controlled on-site delivery of Li-ions to the metal surface, leading to a uniform Li deposition. Further suppression of Li dendrites will be obtained by high mechanical stability of GO acting as physical barrier; from ref.[77].

2.3. Chemical modification related to ionic conduction

The chemical reactivity of GO relies essentially on O_f that, *a priori*, behave like in any organic compound.[81,82] Table 1 gives an overview of the possible reactions related to the type of O_f taken from the recent review by Guo et al.[80] and Fig. 6 is an illustration of the different chemical reactions that can be performed. In addition to this high level of functionality, the good dispersibility of GO in various solvents makes its chemical modification relatively easy to perform.

O_f are determining for the interaction/association of GO with the polymer matrix to which it is added. Van der Waals interactions are also frequently used for a non-covalent modification of GO.[81] This avoids a synthetic step costly in time, in energy, and in chemicals. Therefore, covalent binding of a functional moiety on GO should be duly justified, for example the grafting of E-containing specific functions (E = B, N, S, F…). Another reason is to bind chemicals that would otherwise migrate, segregate or evaporate over time. The objective is to achieve the highest level of homogeneity and stability over time, for example to avoid stacking or restacking of GO layers. Let's emphasize that a general problem is the quantitative determination of the level or degree of modification. As it can be difficult to determine, it requires additional efforts from researchers.

Esterification of carboxyl group is among the simplest example of covalent chemical modification reported in the field of batteries, the carboxylic group being directly esterified with OH-terminated PEG or PEO by direct mixing of GO, for example methoxy-polyethylene glycol (M_w = 350 g mol^{-1}) at 60 °C for 12 h in acidic conditions.[83] In another work, activation of –CO_2H by $SOCl_2$ was preferred prior to esterification with PEG[84] or with boric acid.[85].

Amidation of carboxylic group can be obtained with an amine but the activation of the carboxylic group requires the use of a coupling agent such as DCC,[86,87] EDC,[88,89] or TPP-4DMAP in pyridine.[90].

Epoxides on GO react by ring-opening with an amine and lead to prepare different imidazolium-containing GO for solid state hybrid electrolytes.[91,92] The same reaction with 3-amino-1 propane sulfonic acid is a way to introduce -SO_3H group.[93,94] Although easy to perform in basic conditions, the possibility of parallel reactions with

Table 1
What can be done with functions on GO; other information can be found from ref.[80].

Target functional group	Reaction	Advantages	Limitations
Epoxide	Nucleophilic ring-opening	Mild conditions	Risk of partial reduction of GO when using basic nucleophiles
Hydroxy	Silanization	Large choice of silane	No use of amino-terminated or thio-terminated silane
	Chlorosulfonic	Well established to prepare sulfated GO	Use of water-free solvent
	Boronic acid Esterification	Mild condition Large choice of carbocylic reagent	Limited grafting level
	Carbamatisation	Mild conditions	Possible side reaction with carboxylic function
	Williamson reaction	Mild conditions	Avoid high pH
Carboxyl	Esterification	High chemselectivity	Limited grafting level
π-bound	Diazotation	Large compatibility with other functions	Oligomerization as side reaction

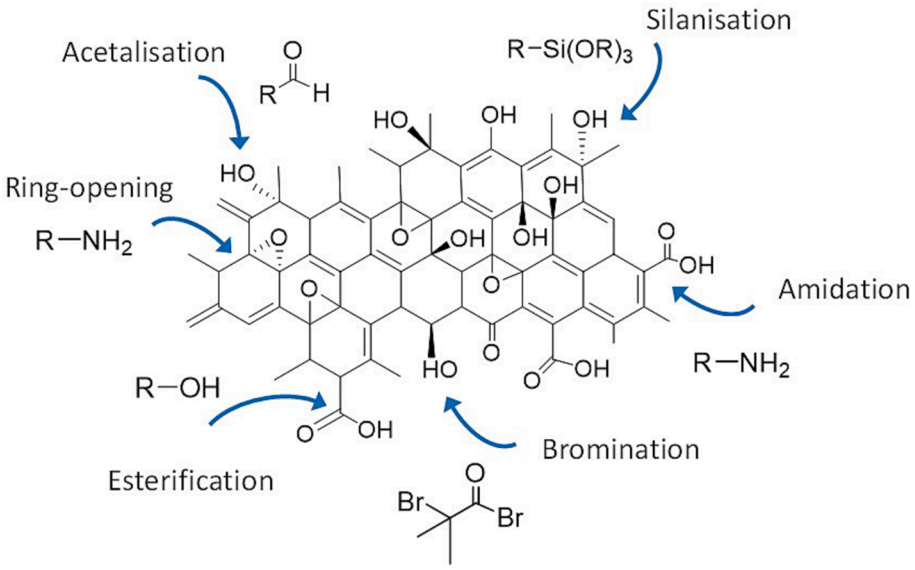

Fig. 6. Illustration of some chemical modifications in view of the use of GO for application in batteries (esterification amidation, epoxide-RO, chain growth …).

other functions on GO like aldehyde, ketone or even carboxylic acid depending on the pH should be questioned.

To increase the homogeneity of polymer/GO blends and definitively avoid any stacking of GO, polymer chains can be grown from specific function on the surface of GO. To this end, either a polymerizable group or an initiating function is first generated on GO surface. For example, the polymerisation by reversible addition-fragmentation chain transfer (RAFT) of (ethyleneglycol)methylethermethacrylate was initiated from sulphur functions, resulting from the treatment of GO by S-(thiobenzoyl) thioglycolic acid.[95] In other studies, polystyrene-based chains were grown from GO by oxidising OH-group with Ce(IV), generating oxygen radical that launch the vinylic polymerisation of 1′4-vinyl(R)aromatic (R = SO_3H or Cl).[96,97] A last example is the growth of hairy polyacrylamide chains via radical polymerization by atom transfer from C-Br functions onto GO, the latest being obtained by bromination of alcohol functions with α-bromoisobutyryl bromide.[98].

Silanisation, by means of the reactivity of the –OH group towards the Si-O-R and Si-OH groups, allows the grafting of already-made SiO_2 nanoparticles,[99–101] or their growth with $Si(OEt)_4$ as precursor.[102] Silanisation is also used to introduce organofunctional groups such as propyl-ammonium function, for example dimethyloctadecyl-[3-(trimethoxysilyl)propyl]ammonium chloride.[103].

Alcohol functions can also react to form acetal, for example with glutaraldehyde, which has been used to cross-link GO layers either with itself or with another OH-bearing functions like cellulose. [103].

Finally, we can mention that carboxylic and alcohol groups are probably also involved when grafting inorganic particles of WO_3 with Na_2WO_4 as precursor.[104].

3. GO and commercial separator

A separator is a macroporous membrane separating the electrodes and impregnated with liquid electrolyte. Synthetic organic (polypropylene, polyethylene, polycarbonate) or inorganic materials (silica) as well as biopolymers (cellulose) are mostly used. Their mechanical and surface properties are determining for the overall performance of the battery.[105–107] Separator must be chemically and thermally stable with enough mechanical resistance to withstand manipulation and deformation. Most importantly, a uniform porosity and wettability are key parameters. A polymer separator typically increases the resistance of the electrolyte by a factor four to five. This technology is well identified by manufacturers and a specific interest is brought to the design of a separator which would control the SEI, would slow down the dendritic growth and polysulphides. Two approaches can be distinguished, represented in Fig. 7, one based on the surface modification of a commercial separator with GO, the other aimed at developing new separators incorporating GO. Below, we consider both approaches but only when the treatment of these separator is sub-micrometric in size, considering that thicker treatments better fit in the “Thin layer with GO” section.

3.1. Chemical modifications of commercial separator

Celgard separator made of a polyethylene layer sandwiched between two outer layers of polypropylene (↕ ~25 µm, Fig. 8a) presents uniformly distributed slit-like submicronic pores (size < 100 nm). Its olefinic nature may seem not adapted when considering cation conduction processes.[108] It is however very popular, due to its inertness and stable association with the polar electrolyte. GO has soon been explored to increase its surface polarity and wettability. A ‘pre-wetting’ by alcohols (generally isopropanol), allows forming a GO nanocoating (↕

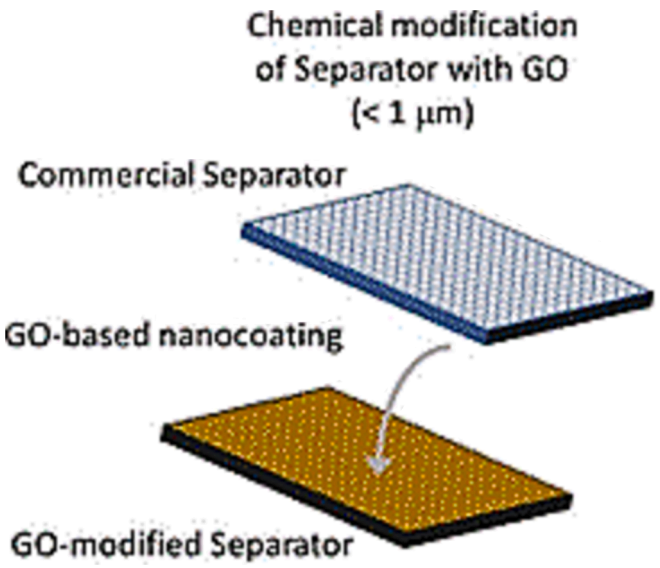

Fig. 7. Representation of the Assembly or modification of a commercial separator by GO.

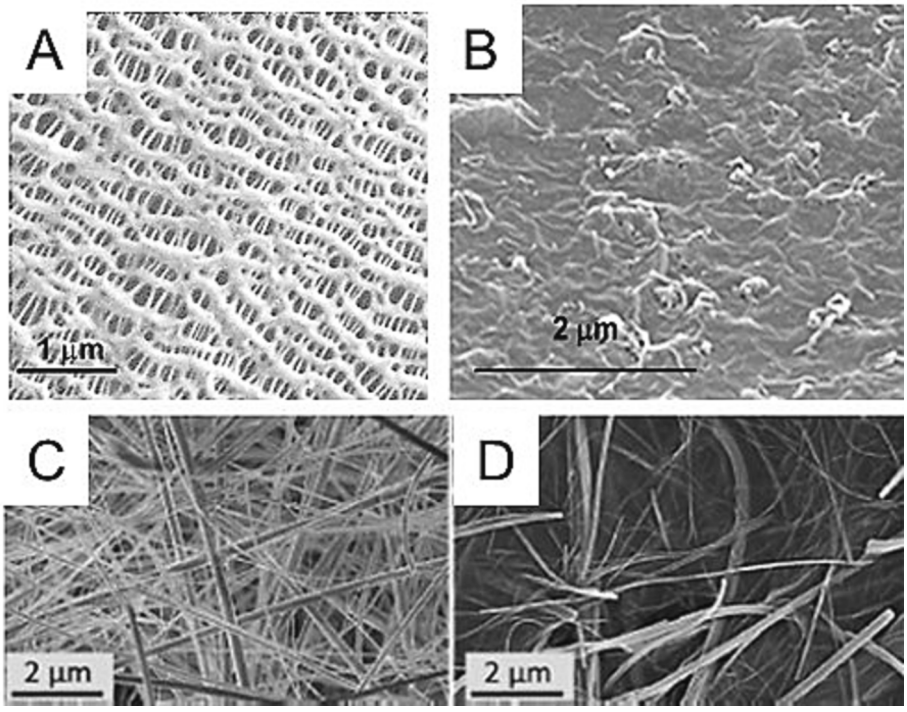

Fig. 8. Microstructure of commercial separators observed by SEM: a/ the pristine Celgard separator, b/ the GO/o-CNT separator, reprinted with permission from ref.. [112] copyright (2015) c/ the pristine Whatman® separator and d/ the GO/PVDF-modified separator; reprinted with permission from ref. [77] copyright (2018)

~30 nm) by direct filtration of a GO suspension on the separator.[109] However the strength and stability over time is questionable in the absence of covalent bonds between GO and the separator. To avoid such questions, GO is frequently associated with a polyolefin-compatible polymer, for examples with PVDF[110] or Nafion^{TM}.[111].

For Li-S battery, Zhi *et al.* first reported the spray-coating of the Celgard separator with a suspension containing GO and oxidized CNT forming a submicron-thick layer (0.3 mg cm^{-2} GO/CNT 50/50 wt%), as illustrated in Fig. 8b.[112] Improved performances were ascribed to the limitation of the S_n^{2-} migration. Zhang *et al.* also observed such an effect but with a nanocoating of Nafion^{TM} (↕ 100 nm) and GO (↕ 30 nm) covering the macropores on the separator, able to "physically" suppress the S_n^{2-} while O_f of GO and -SO_3^- of Nafion^{TM} enhance Li^+ hopping as illustrated in Fig. 9.[111] More recently, similar improvement of Li-S battery was reported for GO associated with Co-phthalocyanine (5 µg cm^{-2}, ↕200 nm),[113] with nanocellulose,[114] or with MgAl layered double hydroxide nanosheet that, in this latter case, leads to a very low capacity decay of 0.08 % per cycle over 500 cycles at 0.2 C and a high reversible capacity of 608 mA h g^{-1} after 100 cycles at a high sulphur loading. [115].

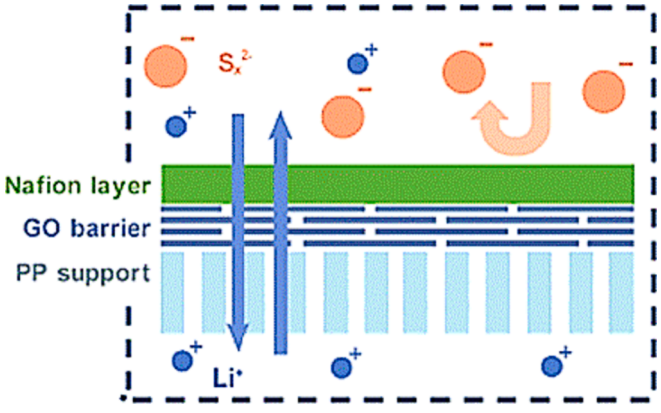

Fig. 9. Illustration of the effect of GO on Celgard separator; reprinted with permission from ref.ef [111] copyright (2016)

Celgard was also efficiently modified with GO-based nanocoating to improve its performance in other types of batteries such as Li-Anthraquinone (↕ 905 nm, 0.1 mg cm^{-2}, GO/Super P 33/67 wt%), [116] Li-LFP (↕ ~900 nm, 0.07 mg cm^{-2}, GO/Prussian blue/Poly-acrylonitrile 31/60/9 wt%)[117] and Li-Cu(TCNQ) (↕ ND, 0.13 mg cm^{-2}, GO).[118].

Whatman® separator, generally named GF, is the other commercial and popular separator made of randomly arranged borosilicate glass fibers (∅ <2 µm, Fig. 8c), it is much more porous (66 %, ~0.6 < pore ∅ < 0.8 µm) than Celgard (41 %) although thicker than it (↕ 250 µm). Compared to Celgard, adhesion of GO on silica-based material is certainly stronger and more stable, ensured by H-bonds between –OH function or even Si-O-GO link. By spray coating,[77] Shahbazian-Yassar *et al.* prepared a GF separator by depositing 1.0, 0.5 or 0.2 mg cm^{-2} of GO mixed with PVDF (GO/PVDF ND/ND wt.%, Fig. 8d). The uniform deposition of Li during plating/stripping and the inhibition of dendrite is ascribed to "defect sites" and to negatively charged functional groups on GO along with its high mechanical stability. Interestingly, Celgard treated in the same condition led to lower electrochemical performance.

GO was associated with some other separators, in the case of an Li-$LiCoO_2$ cell, a GO/PVdF-HFP coating on a "manufactured PET nonwoven substrate" improves performance for an optimal GO-concentration 0.0066 wt%, but "PET" structure is not defined.[119].

Conclusion on Modification of Commercial Separator with GO – This strategy is acceptable for production processes. It consumes low quantities of reagent and occupies a limited volume. In addition, from a single commercial separator, different direct treatments (spray-coating or filtration) allow addressing specific solution to each type of battery.

3.2. Elaboration of new separators with GO

To elaborate a porous separator, blading of a slurry followed by phase inversion in a non-solvent is a relatively simple process. As an example, an acetone/DMF solution of PVDF/Al$(H_2PO_2)_3$/GO (33/66/

0,01 wt%) after phase inversion (to ethanol) and wetting with liquid electrolyte ($LiPF_6$/EC/DEC/DMC/VC) were carried out for preparing a separator with high porosity (51 %, ↕29 μm) and offers in Li-$LiNi_{0.8}Mn_{0.1}Co_{0.1}O_2$ batteries a high capacity up to 188.8 mAh/g at 0.2C and a retention capacity of 82.2 % *versus* 41.4 % for Celgard after 200 cycles.[122] GO also improves the.

performance of PVDF-HFP-based separators prepared by direct casting (Fig. 10a).[120] For an optimum GO content of 0.1 wt% (↕ 130 μm, pore size distribution 5–200 mm and 10–400 nm, porosity of 65.3 %) this separator in Li-LFP battery led to a capacity (160 mAh/g) 37.9 % higher compared to pure PVDF-HFP (116 mAh/g) and 19.4 % higher than Celgard (134 mAh/g).

For a separator made of a poly-hyperbranched-PEO assembled with GO, porosity was introduced by soft templating using a colloidal polystyrene suspension. Although the electrochemical performance in Li-LFP cells are somehow interesting, a separator without GO was not reported as a control and the wt.% of GO not given. It is thus not possible to highlight the contribution of GO in this case.[73].

However, the most recent approach of elaborating new separators is the electrospinning of GO-containing fibers forming a non-woven mat with adaptable thickness and diameter of the fiber. PEO-based fibers were electrospun from GO/PEO/EC/$LiClO_4$ suspension in acetonitrile (GO content 0.07 – 0.35 wt%, 300 < ∅ < 800 nm).[123] An interesting comparison with similar MWCNT-containing fibers points to a higher ionic conductivity when using GO as filler (up to $\sigma = 0.057\ 10^{-3}$ S cm^{-1}) but a slightly higher transference number when using MWCNT (up to $t_{Li+} = 0{,}51$). A situation quite disturbing when considering the huge difference of functionality and structure between GO and MWCNT and that questions the "cooperative process between O_f at the GO surface" that is frequently claimed in publications. In addition, even perfectly unstacked, the very low proportion of GO (0.5 to 1 wt%) corresponds to a very small proportion of PEO in interaction with the GO interface and very small volume fraction of the SPE for Li^+ to migrate.

For PVDF-based fibers electrospun from a PVDF/GO/TiO_2 solution (400 < ∅ < 650 nm, GO-content 1, 2, and 3 wt% and TiO_2-content 5 wt %), the presence of GO clearly led to higher electrolyte uptake (up to 490 %) and σ (up to $4\ 10^{-4}$ S cm^{-1}).[124] For interested readers, a comparison can be made with a rGO/PVDF electrospun separator.[125].

Polyacrylonitrile is the most studied in this field, it is easy to process, it offers excellent resistance to oxidative degradation and cyano groups are potentially efficient to bind Li^+ leading to homogeneous ionic conduction hindering dendrite growth.[126,127] Electrospun PAN fibers (∅ ~210 nm) were covered with a thin layer of a doubly oxidized GO (HGO) by filtration (↕ 5 μm), the average pore size diameter ~ 520 nm of PAN fibrous mat (↕ 35.0 μm) is reduced to 223 nm by HGO resulting in improving resistance to dendrite growth (Fig. 10b).[121] Direct electrospinning of PAN/GO suspension (91/9 wt%) gave fibers (600 < ∅ < 850 nm) and mat having high porosity (70 %), high wettability (300 % of liquid electrolyte uptake) and improves performance of Li-S battery (capacity of 597 mAh/g after 100 cycles, 38 % higher than with Celgard separator). This was ascribed to the specific role of –C≡N in binding polysulfides and to electrostatic repulsions between negatively charged GO and polysulfide S_n^{2-}.[128] In a Li-LFP battery, polyacrylonitrile-co-vinylacetate/polymethylmethacrylate/GO mat (99/11/2 wt%, fiber ∅ ~130 nm) led to attractive performance: $t_{Li+} = 0.77$, $\sigma = 1.5 \times 10^{-3}$ S cm^{-1} at 30 °C and high discharge capacities (155 mAh/g at 0.1 C, 52 mAh/g at 2C). Noticeably, here also GO was prepared by a double oxidation process.[24].

Hydrolysis of the nitrile groups followed by esterification with alcohol functions on GO was performed to ensure a covalent bonding between PAN and GO.[129] The resulting electrospun mat (GO-content 10 wt%, ∅ = 200—300 nm, mat ↕130 μm) had good ionic conductivity ($\sigma = 4.53\ 10^{-3}$ S cm^{-1}), transference number ($t_{Na+} = 0.70$, $t_{Li+} = 0.64$) and improved C-rate capacity compared to PAN and commercial Celgard separators in Na-$Na_3V_2(PO_4)_3$ and in Li-$Li_4Ti_5O_{12}$ cells.

One can also mention that electrospun fibers with polyurethane [130], polyurethane/polyvinylpyrrolidone[131], polyimide[132,133] or PVDF-HFP p/poly-m-phenyleneisophthalamide (PMIA)[134] were also reported, but the absence of precise structure of these polymers severely limits the usefulness of the data.

Conclusion on Elaboration of New Separator with GO – Electrospinning offers the possibility to vary the composition, fiber diameter and mat thickness and is well suited for upstream research. What's more, the flexibility of this technology and the ability to produce membranes on a large scale make it competitive with commercial separators.

4. GO in coating and thin layer

The terms "interlayer" or "protective layer" or "film" or "coating" or "artificial SEI" generally refers to a submicron to micron-size layer (↕ >1 μm) covering either the surface of the separator or the electrode. Here, we will abbreviate all these different situations by TL for Thin Layer. This very broad scope concept is basically depicted in Fig. 11. Thicker film, in absence of commercial separator, are considered in the solid-state electrolyte section.

To modify the properties of the separator, various polymer-based or inorganic-based protective layers have been reported and can effectively stabilise the Li interface,[11,135] or block the sulphides migration in the specific case of Li-S battery.[136,137] Below, we differentiate the case of the protective layer when it is coated on the separator, the anode or the cathode.

4.1. Thin layer combined with separator

In 2014, Hammond *et al.* used a layer-by-layer approach to form a non-porous protective multilayer TL (↕ 0.4–4 μm) on Celgard with alternating GO, PEO and PAA layer, with or without LIBOB. The nano-layer of GO was reported to increase the Li-transfer number, decrease

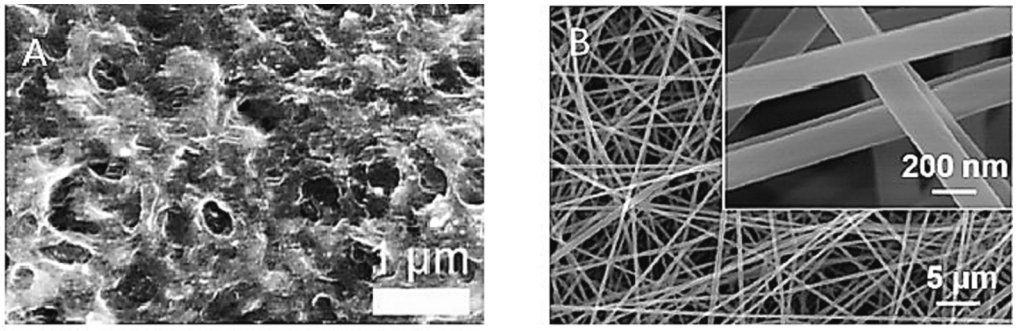

Fig. 10. Example of microstructure of the two main types of separators observed by SEM and prepared either a/ by phase inversion of a GO/PVDF-HFP mixture; reprinted with permission from ref. [120] copyright (2020) and b/ by electrospinning of GO/PAN mixture; reprinted with permission from ref.[121] copyright (2022).

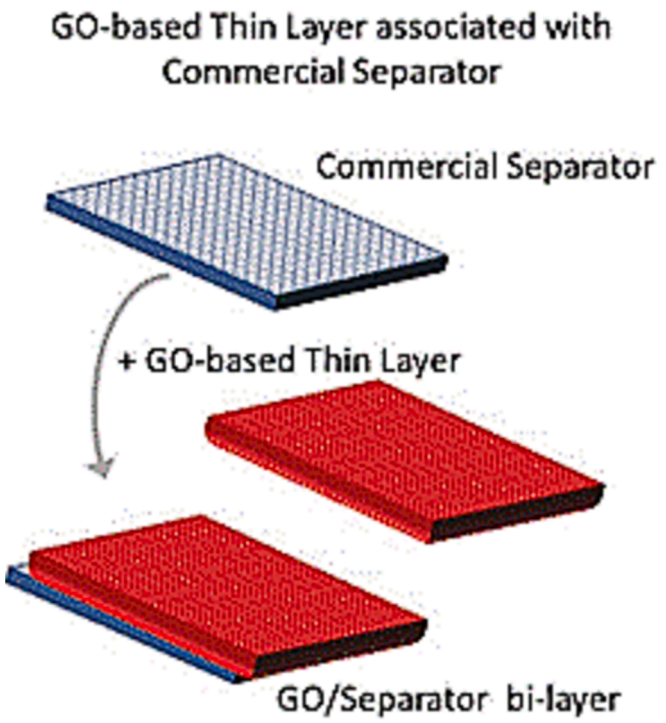

Fig. 11. Representation of the thin layer made of a GO-containing composite deposited on a commercial separator.

the ionic conductivity and the electrolyte permeability of the whole set. Nevertheless, a chrono-potentiometry test indicates a short-circuit time multiplied by 4 with GO and an increase in the Young modulus, that is assumed to explain the resistance to perforation by Li dendrite.[138].

In Li-S battery, the TL technology has been largely developed to prevent the polysulphides shuttling by using carbon-based materials. Graphene oxide is a good candidate and a thin layer (↕ 4–6 mm, 0.4–0.12 mg cm^{-2}) of GO alone deposited on Celgard by direct filtration was reported to efficiently block the polysulfides, this occurring within the very upper part of the layer (5–15 nm).[109].

Many different GO-containing composites have been reported and listed below according to their chronological publication: GO/MWCNTs (1.1 mg cm^{-2}, ↕~30 μm on Celgard),[139] GO/PVDF (91/9 wt%, ↕18.3 μm on Celgard),[140] aligned MWCNT GO (↕ 2 μm, density 0.10 mg cm^{-2}, GO content 0.05 mg cm^{-2}, on Celgard),[141] GO/CNC,[142] GO/polyaniline paper (↕ 9 μm, PANI-content 2.48 mg cm^{-2} on Celgard),[143] GO/SiO_2/CMC (100/3/0.08 wt%, ↕<5μm on Celgard),[144] GO/CaF_2/Ketjen black/PVDF (8:1:1 wt%, ↕ND, on PP membrane, 0.15 mg cm^{-2}),[145] GO/polyaniline deposited on MWCNT (GO layer ~ 700 nm, MWCNT mat > 3 μm, GO facing the cathode on glass fiber separator),[146] GO/PAN (1:10 wt%, electrospun PAN nanofibers ∅ ~640 nm, ↕63 μm on glass fiber facing the cathode),[147] GO/PVDF (GO 0,1; 0,2 and 0,5 wt%; electrospun PVDF fiber ∅ ~1 μm; 2–40 μg cm^{-2}, ↕5 to 10 μm on Celgard),[110] GO/poly1,5-diaminoanthraquinone (20/80 wt %, ↕40 μm on glass fiber separator),[148] $BaTiO_3$-GO/PVDF (80/20 wt %, ↕25 μm on Celgard).[86].

In a study on a GO/nanocellulose composite as interlayer on Celgard, GOs with different oxidation degrees were prepared by playing on the time of graphite oxidation by $KMnO_4$, leading to a high level of epoxide functions. Electrochemical tests evidenced an improvement of the specific capacity for the less oxidized GO but limited to the first 100 cycles, and a detrimental effect of a too oxidized GO but interpretations not straightforward and unfortunately, information on the cellulose itself are missing.[149] Another interesting comparison has been made between thin films (↕ ~40 μm on Whatman ↕260 μm) of GO-based composite including either SiO_2 or TiO_2 or PDAAQ (80/20 wt% in each case).[148] In all cases, the performance of the Li/S battery was improved by the TL and GO/PDAAQ gives the best performance in terms of cyclability, coulombic efficiency and blocking of polysulphides.

This TL technology is also tested in other battery like: Li-LCO (a GO/SiO_2/CMC film 100/3/0.08 wt% and ↕<5 μm on Celgard)[144] or Li-$Li_4Ti_5O_{12}$ (GO-PAM/PVDF 80/20, ↕ND on Celgard).[98].

For Li-O_2 battery,[150] a synergistic effect between the three components PSS-Li, GO-Li and SiO_2 (4, 10 and 15 wt%, ↕67 mm, on glass fiber) has been demonstrated to prevent the shuttling of redox molecules such as TEMPO from catalyzing the cathodic reactions: $2Li^+ + O_2 + 2e^- \rightarrow Li_2O_2$. Similarly, TL of pure GO (200 nm, 0.01 mg cm^{-2}, on PTFE membrane) prevents the migration of 5,10-dihydro-5,10-dimethylphenazine, a redox-mediator required for oxygen reduction.[151].

For Zn-ion battery,[79] Zhang *et al.* obtain a thin layer of GO (↕ 10–20 μm) by direct filtration of GO solution on a GF separator (Fig. 12). Among different effects, the GO layer clearly reduces the interfacial charge-transfer resistance during platting/stripping. It is also demonstrated that the ionic conductivity of the GF is improved by the GO layer (up to $\sigma = 0.014$ S cm^{-1}) resulting in high electrochemical performances in Zn/MnO_2 cell. In that case, the suppression of dendrite was not ascribed to the mechanical strength of GO but to specific interaction with Zn as explained in the above section. In the same publication, authors report similar improvements in Li symmetrical cell, but without evidence of any effect of GO on Li similar to the one on Zn.

In an aqueous battery like C-Na_x[$FeFe(CN)_6$], GO (↕ ~7–8 mm on GF separator) improves the retention of capacity (78.8 % after 10 cycles for a current density of 2 A/g) thanks to sieving effect; the hydrated $Fe^{3+}_{(aq)}$ (∅ of 9.6 Å) being blocked by the interlayer nanochannels ~1 nm contrarily to the hydrated $Na^+_{(aq)}$ (∅ of 7.2 Å) whose migration is required.[152].

4.2. Thin layer on anode

According to DFT calculations, the adsorption of Li near GO defects is a thermodynamically favoured process leading to an initial deposition of a thin layer of Li on the GO sheets.[153] Before this theoretical confirmation of the lithiophilic character of GO, a uniform and continuous GO coating on $Li_{(s)}$ was obtained via simple wetting with a DMC solution, Fig. 13.[154] Furthermore protective layers with GO on anode aims to avoid direct contact of liquid electrolyte with Li and/or to modify the SEI, example of this are: GO/black phosphorus in a Janus bilayer structure in Li-S and Li-LFP batteries (↕ 500–1000 nm),[155] GO/PVDF-HFP/PEGA (13/26/48,6 wt%, ↕8–9 μm) in Li-Li and Li-LFP cell,[62] GO/P(SF-DOL) (20/80 wt%, ↕3 μm) in Li-$LiNi_{0.5}Co_{0.2}Mn_{0.3}O_2$ cell.[156].

A GO-containing layer was also investigated to stabilise the Li surface in contact with an inorganic electrolyte like Li_6PS_5Cl when tested in LCO battery (GO/H_3PO_4/ECel: 8/80/12 wt%, ↕33 μm).[157] Prevention of dendrite growth, limitation of polysulfide migration and improved stability are generally ascribed to different reasons: the mechanical properties; a filling-in effect to smooth the surface; or an impermeabilization avoiding direct contact of Li with liquid electrolyte. An outstanding question is an increase in the reduction of GO in contact with Li while combined with other chemicals of the SEI.

In the specific case of Li-O_2 battery, a GO/SiO_2 composite was proposed to protect Li from corrosion.[101] Interestingly, GO/SiO_2 compositions present an optimum, the best result being obtained with a 2/1 mass ratio (↕ 22 μm) that was conveniently deposited by drop casting. In this case, the battery reaches at least 348 cycles at 1 A/g, with 1000 mA h g^{-1} of capacity, much more than a coating with either GO or SiO_2 alone.

To avoid treating a reactive metal like lithium, it would be easier to treat the Cu collector combined with a first plating that will produce Li between the Cu collector and the protective layer. This was reported in the case of spin-coating of GO on Cu collector (~0.134 mg cm^{-2}), using a liquid electrolyte with 5 % fluoroethylene carbonate to generate an

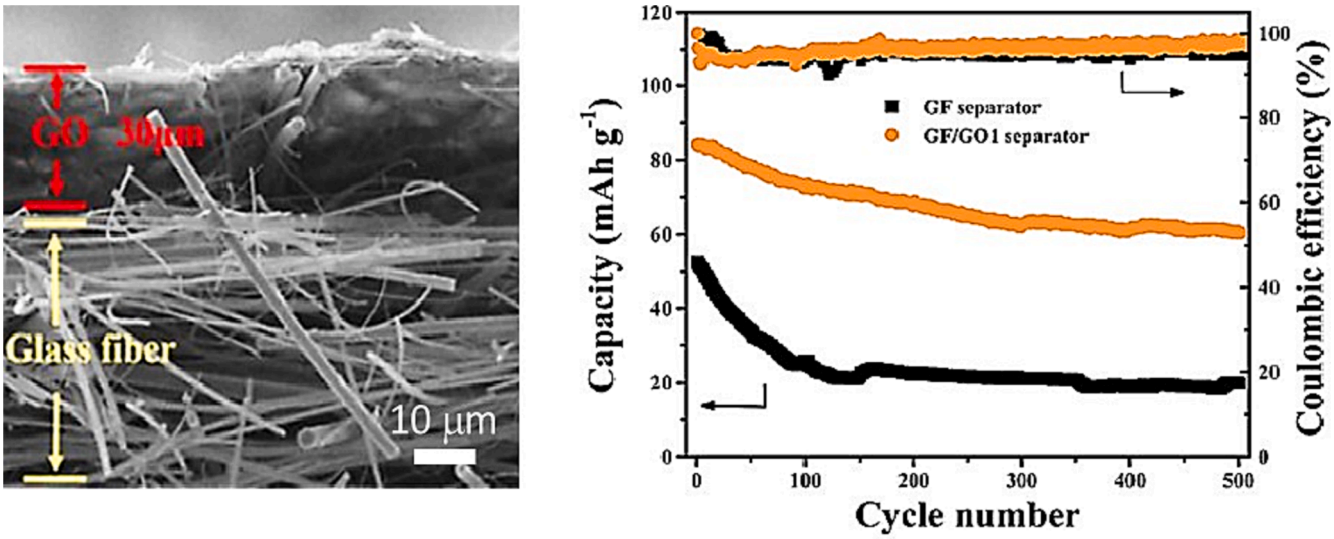

Fig. 12. A/ example of a thin protective layer on a GF separator and B/ its performances in a Zn-MnO_2 cells with GF and GO/GF separator at a current density of 0.5 A/g; reprinted with permission from ref.[79] copyright (2020)

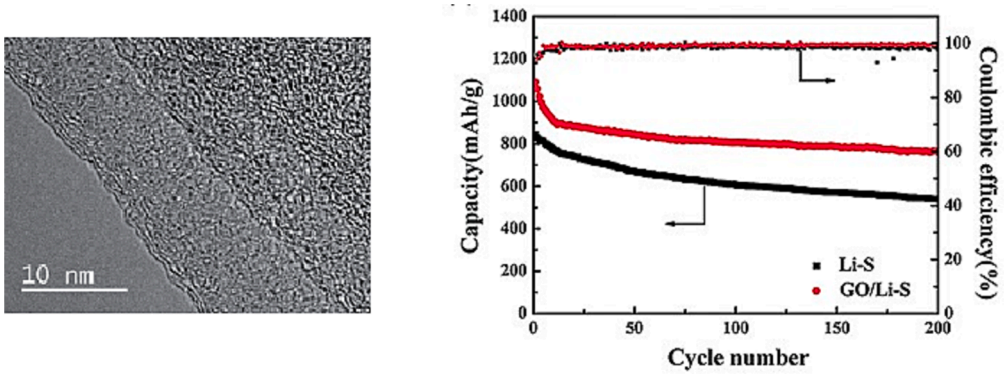

Fig. 13. TEM images of Li covered by ultrathin GO layer and performance of the corresponding Li-S battery; reprinted with permission from ref.[154] copyright (2016)

LiF/GO-rich SEI on Li that improves the life-time and coulombic efficiency of Li-$LiNi_{1/3}Mn_{1/3}Co_{1/3}O_2$ battery.[158] Such effective treatment of the current collector works also for Mg-metal battery, another electrode material candidate for new generation of batteries. Corrosion/passivation of the Mg interface and electrolyte oxidation was prevented, at least partially, by electrodeposition of the GO layer (↕ 200 nm, 60 μg cm^{-2}) on Al or Cu collector up to 4.0 V and without negative impact on plating/stripping of Mg. It was demonstrated that the O-rich function on GO is a key factor in this process since a rGO coating does not offer the same protection.[159] Additional data on the prevention of Mg corrosion were reported recently.[160].

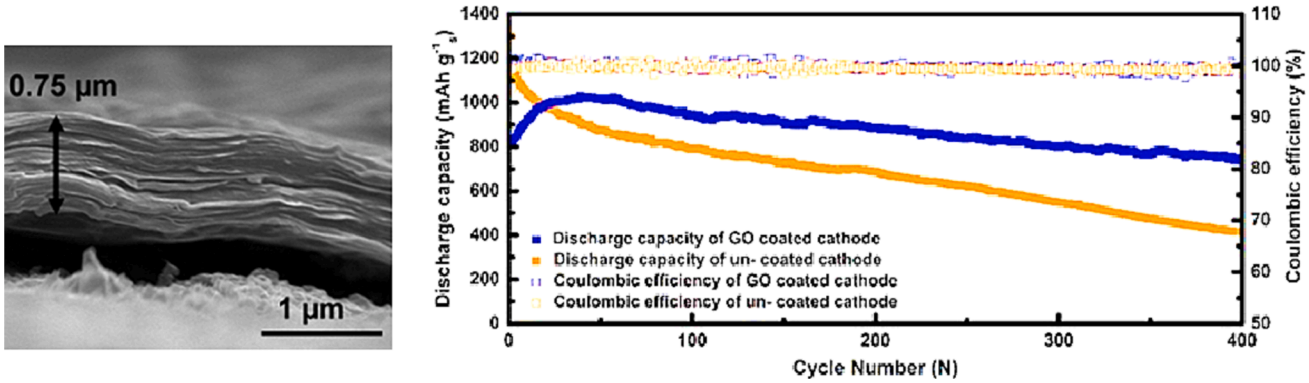

Fig. 14. Structure a GO coating on the sulphur cathode observed by SEM and long-term cycling performance of Li-S battery with sulphur cathode at 1C rate with and without the GO membrane; reprinted with permission from ref..[161] copyright (2016)

4.3. Thin layer on cathode

For Li-S battery, numerous publications report the formulation of the sulphur cathode with GO, generally further reduced in rGO, but this is not the topic of the present review. Instead, or more likely in combination with this, a thin GO layer on top of the sulphur cathode was deposited by simple blading (↕ 0.75 μm) and leading to improved electrochemical performance (initial discharge capacities of 1182 mAh/g for electrodes with 80 % sulphur content at a 0.5C rate and a capacity of 835 mAh/g after 100 cycles at 0.5C, Fig. 14).[161] Recently, an easy way to process GO/sulphur-carbon/MXene cathode led to a specific capacity of 1425 mAh/g at 0.1C in the initial cycle and a cyclic retention of ~85.1 % after 500 cycles.[162].

Conclusion on TL technology - Some general remarks to point out: 1/ the additional layer associated with the separator is generally effective to improve the performance of the battery, although it often results in higher polarization voltages due to their relatively high resistance; 2/ the most useful studies are those where at least one parameter, especially the composition or the thickness, is screened on its impact on battery performance, allowing to better identify the role of each component in a multicomponents film; 3/ a full characterisations of the GO's evolutions is generally missing.

5. GO in gel electrolyte

An electrolyte gel is a quasi-solid material that frequently consists of three parts: a cross-linked polymer matrix swollen at the molecular level by a liquid solvent, sometime called "plasticizer", at room temperature, in which lithium salts are dissolved, see Fig. 15 for a simplified representation.[163,164] When the polymer bears ionic functions, the salt might not be necessary. Both the polymer and the liquid must have high polarity and dielectric constant to allow dissolution and dissociation of salt ions. In addition, high thermal stability and good chemical stability are required to prevent secondary reactions, especially in contact with electrode materials.

To prepare gel polymer electrolyte (GPE), the most used polymers are PEO, PVA, PMMA, PAN, PVDF, or PVDF-HFP swollen in classical plasticizers such as carbonate (EC, EMC, DMC, DEC, PC), ether (DOL, THF, DME), amide (DMF) or sulfoxide (DMSO). The salt is frequently $LiClO_4$, $LiPF_6$, LiBOB, or LiTFSI. In this domain, graphene oxide has been used as a filler, sometimes after chemical modifications, that can increase the mechanical properties but also the ionic conductivity.

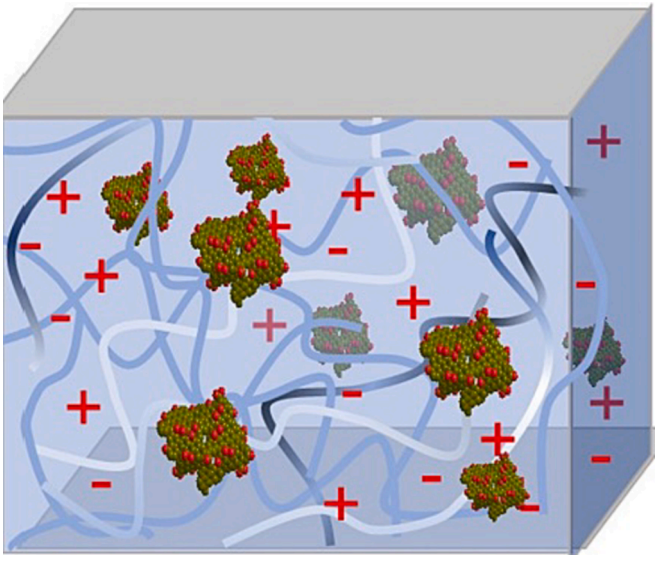

Fig. 15. Representation of a GO-containing composite gel swollen with solvent and Li^+-containing salt.

In some reports, GO is used in a supercapacitor in a gel electrolyte, Chen *et al.* observed a 260 % increase in the conductivity when adding 1 % of GO to a pure PVDF-HFP-2EMIMBF$_4$ gel (GO/PVDF-HFP/EMIMBF$_4$: 1/33/66 wt%, $\sigma = 9\ 10^{-3}$ S cm^{-1} at RT).[165,166] The effect of GO is attributed to amorphization of the P(VDF-HFP), an optimum GO-content ~ 1 wt% being observed in that case and related to the polymer/GO interactions *versus* GO stacking.

For Li-LFP battery, Wang and Gong have compared GO and PEO-modified GO in PVDF-HFP-based GPE: one made GO/ PVDF-HFP LiTFSI/EMITFSI (GO optimum content: 0.3 wt%, $\sigma = 1.3\ 10^{-3}$ S cm^{-1} at 30 °C, $t_{Li}+ = 0.79$, up to 4.85 V)[167] and the other made a PEO-esterified GO (GO@PEO/PVDF-HFP/LiTFSI/EMITFSI, GO@PEO optimum content: 2.4 wt%, $\sigma = 1.6\ 10^{-3}$ S cm^{-1} at 30 °C, $t_{Li}+ = 0.82$).[168] In both cases, GO improves the performance of Li-LFP cell, optimum concentration corresponding to a large decrease in the crystallinity of the polymer. However, the superior Li-LFP cell discharge capacity (+16 % at 0.1C and X 7.5 at 5C) demonstrates the interest of the esterification of GO with PEO that enhances the compatibility with PVDF-HFP and avoids GO stacking. Another chemical modification of GO giving attractive results is the functionalisation with SO_3H-groups. The addition of 3 wt% of a SO_3H-GO to a Nafion^{TM}-based GPE swollen in EC:PC increases the ionic conductivity from 3 to 5 10^{-3} S cm^{-1} at 30 °C, and the transference number is the one of a single ion conductor ($t_{Li}+$ ~0,99).[93] An interesting point of this study is the analysis of the Li^+ motion by ^{7}Li NMR allowing the determination of the diffusion coefficients that represents the long-range motions (~10 nm to ~ mm) and spin – lattice relaxation T_1 that depends on rotational and short-range translational motions in the time scale of the reciprocal of the NMR frequency (~1 nm). Lithium diffusion in the Nafion^{TM} GO-free was found higher than in the presence of GO and "the shorter T_1 values in the GPE with SO_3H-GO confirms that Li^+ is involved in more stringent interactions with the lattice," as explained by the authors.

For Li-$LiCoO_2$ cell, Li *et al.* mixed PVDF with a modified-GO covalently grafted with borate-polyacrylic acid and swollen in 1 M $LiClO_4$-EC/PC/DMC (Fig. 16).[85] Here, the optimum GO-content is much higher than in other GPE ~ 10 wt% but leads to a fairly ionic conductivity $\sigma = 3.82\ 10^{-3}$ S cm^{-1} at 25 °C, a large stability window (~4.7 V), an average transference number $t_{Li}+ = 0.52$ and an attractive discharge capacity. In a different polymer matrix, PTC was selected to prepare a GPE because of its high dielectric constant ($\varepsilon = 50–57$; GO/PTC/PEO:0.1/10/1, swollen with 1.0 M $LiPF_6$ in EC/DEC/FEC).[169,170] Here again, GO slightly improves the ionic conductivity ($\sigma = 2.28 \times 10^{-3}$ S cm^{-1}, +12 %), the transference number ($t_{Li}+ = 0.60$, +33 %) and stability (up to 5 V). Very recently, for polyethylene glycol-based matrix (PEGMA-EGDMA swollen in 1 M $LiPF_6$ in DEC/DMC), the reported effect of GO seems limited although an optimal GO-content of 0.3 wt% gives the best performance for ionic conductivity and a $t_{Li}+$ ~0,6. This GO-content also leads to the highest swelling ratio.[95,171].

In Li-O_2 battery, PVDF-HFP mixed with PEO and GO (94.3/4.7/0.95 wt% swollen in 1 M LITSFI in TEGDMF) gives the lowest conductivity $\sigma = 3.4 \times 10^{-4}$ S cm^{-1} at 25 °C, higher stability window (5.2 V), similar $t_{Li}+ = 0.58$ and good prevention against dendrite growth.[172].

Aqueous GO-containing GPE were investigated for application in Zn-O_2 battery. In formulation with PVA, PAA, KOH and KI, GO improves the electrochemical performance. The reason is ascribed to be the same phenomenon than the one observed for other batteries despite the fact that the shuttling ions are significantly different.[173].

A different type of GPE was obtained recently by swelling light molecular weight PEG (400 g mol^{-1}) with 1.3:2.4-dibenzylidene-D-sorbitol (DBS) as an organogelator and filled with various amount of GO (0.3, 0.5, 0.7, 1, 2 and 4 wt%).[174] The self-organisation of DBS/PEG association in the gel (↕ 50 μm) is disturbed by the presence of GO and besides, variation of the ionic conductivity reaches an optimum value $\sigma = 5.0\ 10^{-4}$ S.cm^{-1} at RT for a GO concentration of 0.5 wt%.

Very recently, a gel polymer electrolyte (GPE) for solid state supercapacitor was prepared by an easy casting process from aqueous solution

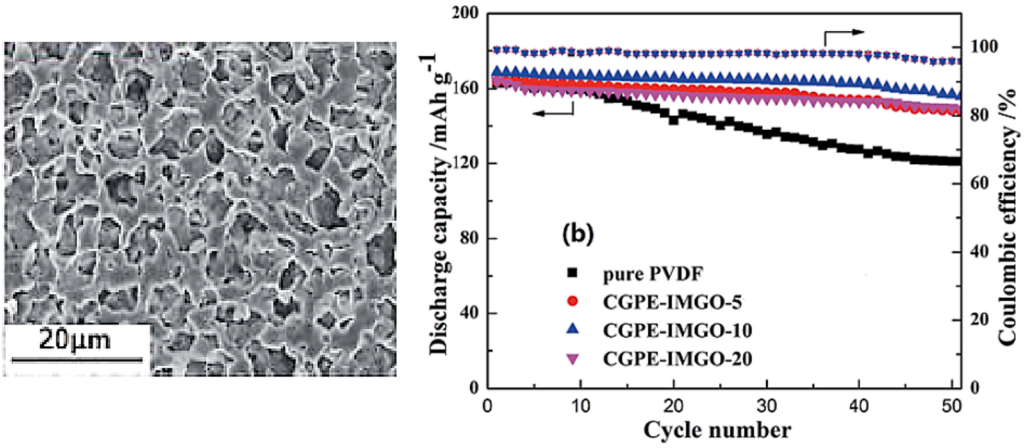

Fig. 16. SEM images of the dried PVDF/GO gel polyelectrolyte covalently grafted with borate-polyacrylic acid (CGPES) and cycle stability and columbic efficiency curves of Li/GPE/$LiCoO_2$ cell; reprinted with permission from ref..[85], copyright (2016)

of agarose as a matrix and GO as a filler (Agarose/LiOAc/GO (100/ 40/ 120/x x = 0,4 0,8, 1,2, ↕800 μm). The amount of water in the gel is not clear but a high ionic conductivity is reported σ = 73.8 mS cm^{-1} with other mechanical and thermal performance.[175].

Conclusion on GEP technology - Some general remarks: 1/ studies of the electrochemical performances as a function of the swelling level are generally never reported but would be interesting for understanding the behaviour of these material; 2/ although an optimum for GO-content is generally observed, it also clearly depends on the matrix and salt composition; 3/ GO has always important effect on the mechanical properties, crystallinity of the polymer and the electrolyte uptake; 4/ elucidation of the structure by CryoTEM and SAXS tool would be useful although generally never reported.

6. GO in solid-state electrolyte

Solid-state electrolytes (SSE) can be either an inorganic (ISE), or a polymeric (SPE) or hybrid inorganic and organic (HSE); in almost all the cases, GO is used as a filler of an organic polymer together forming an SPE. Often, the SPE is immersed in a liquid electrolyte solution before being used and it is difficult to identify to what extent the SPE has been swollen by the liquid and resulting in a kind of borderline situation between SPE and GPE (see previous section).[176].

Reported GO-containing SPE combine pristine or modified GO with PEO or many different polymers and frequently a lithium salt as simply represented in Fig. 17. To the best of our knowledge, GO has never been combined with inorganic conductors such as oxides, sulphides, and halides that possess high ionic conductivities of 10^{-4} to 10^{-2} S cm^{-1} at room temperature and Li-ion transference numbers close to unity but suffer from non-deformability and/or poor stability in ambient conditions.[2,177].

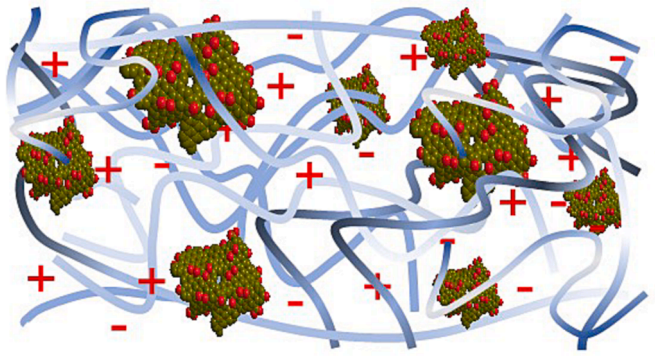

Fig. 17. Representation of a GO-containing composite SPE with including a Li^+-containing salt.

6.1. Pure GO as SPE

To the best of our knowledge, GO alone has only been reported by Qu *et al.*, pressed into tablet (↕ ~30 μm) and sandwiched between two Celgard separator for test in Li//LMO battery.[63,64] The interesting point is that they assumed the possibility to "etch" the grown Li dendrite by oxidation with GO which thus acts as a physical barrier but also as a reducing agent. Unfortunately, characterisations of the GO tablet are not reported (σ, t_{Li+}…).

6.2. Unmodified GO in PEO-based SPE

The history of SPE begun with the report of Wright *et al.* of highly crystalline PEO/M^+ complexes (M = Na, K),[178] Armand *et al.* proposed to use such phenomenon for the elaboration of SPE for Li-batteries,[2,3] and pioneered the ionic conductivity of PEO/salt systems.[179] PEO-based SPE present high flexibility, facile manufacturability, excellent conformability, and low density, but much lower room-temperature ionic conductivities (~10^{-7} to 10^{-5} S cm^{-1}) than conventional liquid electrolytes like carbonate or ionic liquids (~10^{-2} S cm^{-1}). PEO/GO composites were first investigated as membrane for fuel cells,[180] then Ardebili *et al.*[181] and Wang *et al.* in 2014,[182] followed in 2015 by Khan *et al.*,[183] reported separately improvement of the ionic conductivity of PEO/ClO_4 (σ ~ 10^{-7} – 10^{-8} S cm^{-1}) with few wt.% of GO (up to σ ~ 10^{-5} – 10^{-4} S cm^{-1}). The discrepancy between the conductivity values reported may result from either the difference of M_w of the used PEO, from the EO/Li^+ ratio, or from the solvent used. Nevertheless, their results agree on several points: 1/there is an optimal GO-content in each case (either 0.6 wt%[182,183] or 1 wt%[181]); 2/ it leads to an increase in conductivity by two orders of magnitude; 3/ GO disrupts the crystallinity of PEO and PEO/ClO_4 complexes and introduces free volume;[182] 4/ a higher concentration is detrimental because of GO restacking. Other benefits of the presence of 1 wt% GO electrolyte is the increase in the tensile strength up to 1.27 MPa (+260 % compared to GO-free SPE) that, in addition to other mechanical properties, allows building flexible LIB.[184].

Wide-angle X-ray scattering and ionic conductivity analyses conducted by Li *et al.* on GO/PEO/$LiClO_4$ composite (10 wt% of GO) highlight the anisotropic structure of SPE cast from solution leading to GO nanosheet essentially parallel to the surface of the film.[74,185] As a result, an anisotropic factor $\sigma_{\parallel}/\sigma_{\perp} = 4$ was determined between ionic conductivity parallel to the surface $\sigma_{\parallel}$ or perpendicular $\sigma_{\perp}$ to it, such phenomena being essentially presents between room temperature and

ca. 65 °C as illustrated in Fig. 18, where 18 A/ shows the effect of few wt. % of GO on the conductivity of a P(EO)12:$LiClO_4$ mixture and 18B/ is a representation of the evolution the structure of the such mixture with and without GO upon heating. However, the ionic conductivity values are somewhat different from those previously reported for such composites.

An interesting comparison between different PEO/Salt/GO SPE, with salt being either CF_3SO_3Li, LiTFSI or $LiNO_3$, highlighted the importance of the counter anion.[186] Whereas LiTFSI and $LiNO_3$ lead to $\sigma \sim 10^{-4} - 10^{-5}$ S cm^{-1}, lower conductivity $\sigma \sim 10^{-6}$ S cm^{-1} was measured for CF_3SO_3Li, a result corroborated by two other phenomena. The first one is the lower level of PEO crystallisation observed for an optimum GO-content of 0.3 wt% with either LiTFSI or $LiNO_3$. Differently, with CF_3SO_3Li as a lithium salt, such level of crystallisation is obtained for a GO-content of 0.5 wt%. The second phenomenon is that the Gutmann donor number values, 16.9 for $CF_3SO_3^-$ anion and 5.4 for TFSI anion, suggesting stronger interactions between $CF_3SO_3^-$ and Li^+ than between $TFSI^-$ and Li^+.

Xu *et al.* recently report that adding 1 % of GO to a PEO-LiTFSI SPE significantly improves the ionic conductivity ($\sigma = 1.54 \times 10^{-5}$ S cm^{-1} *versus* $\sigma = 2.2 \times 10^{-6}$ S cm^{-1} at 24 °C), the electrochemical stability (5 V *versus* 4.3 V), the transference number ($t_{Li+} = 0.42$ *versus* $t_{Li+} = 0.12$) and ultimately performance in Li//electrolyte//Li cells (lower over-potential 27 mV *versus* 80 mV and higher stability on cycling 600 h *versus* 180 h).[187] Performances of such $LiFePO_4$//GO-PEO-LiTFSI//Li battery are attractive: initial discharge capacity is 142 mAh/g at 0.5C, discharge capacity retention and Coulombic efficiency are respectively 91 % and 100 % after 100cycles and specific discharge capacities at different C-rate is improved specially at 1.0C (92 mAh/g *versus* 59 mAh/g).

GO also improved the electrochemical performance of different PEO-based polymer, however, the high level of control over the polymer structure, some of them with very sophisticated structure, does not meet necessarily high electrochemical performance, see for example a star-shape polymer based on triphenylene and six arms made of block poly (methyl methacrylate)-poly(poly[ethylene glycol] methyl ether methacrylate.[188].

GO was also reported to improve the conductivity of PEO-based Na^+-ion conducting SPE PVP/$NaIO_4$[189–191] or PVA/$NaIO_4$.[192] However its effect is lower to the one observed in the case of Li^+ systems, for example, ionic conductivity remaining at $\sigma \sim 10^{-6}$ S cm^{-1}.

The most recent data reported in this field is the impregnation of aerogels of GO with PEG/PEO/LiTFSI for preparing SPE with residual pores (⌀ 15 μm) ([EO]/[Li^+] = 12:1 and optimized GO wt.% = 10).[193] A more uniform and smoother deposition of Li is observed compared to PEO alone however ionic conductivity ($\sigma = 4.12 \times 10^{-4}$ S cm^{-1} at 50 °C), transference number is not determined and performance in LFP|SPE|Li battery is almost similar to a "GO-doping" of PEO.

6.3. Peg-modified & cation-modified GO in PEO-based SPE

Covalent grafting of PEG chain onto GO is possible via different routes, see section on chemical modifications of GO) and has been explored with the objective to achieve a perfect mixing of GO with PEO and to enhance the ionic conductivity. Lee *et al.*[84] investigated a composite where PEG-grafted GO was mixed with a branched poly(poly (ethylene glycol))methylethermethacrylate having hepta(isobutyl)-POSS side group (BCP) and $LiClO_4$. Comparison between material with either PEG-grafted GO or unmodified GO reveals that both fillers improve the ionic conductivity of BCP with optimum wt.% slightly different around 0.2 and 0.5 wt% respectively. Furthermore, while the ionic conductivity is higher with PEG-grafted GO (2.1 10^{-4} S.cm^{-1}) than with unmodified-GO ($\sigma = 1\ 10^{-4}$ S.cm^{-1}), this relatively small increase questions the value of an expensive chemical modification. A very interesting point of this study is that in both cases the higher the wt.% of the filler, the higher the T_g, a situation at the opposite of previously reported data for GO/PEO composites.[181,182] The concomitant increases in T_g and σ at low concentration of filler is not easy to understand. A possible explanation relies in the fact that this also coincides with an increase in the proportion of free ClO_4^- anion determined by FTIR. It is observed that the proportion of "free" ClO_4^- anion is higher with PEG-grafted GO than in the case of GO alone; the PEG chains grafted onto the GO seem more efficient for solvating and dissociating the Li^+ ClO_4^- pair than pure GO. More recently graphene nanoplatelets, not graphene oxide, was covalently linked to PEG400 through their few carboxylic function.[194] Tested as filler of a PEO (9 10^5 g/mol) this clearly reduces the crystallization of PEO, however, compared to an unmodified graphene nanoplatelets, improvement of the ionic conductivity, $\sigma = 2.5\ 10^{-5}$ S.cm^{-1} *versus* 7.9 10^{-6} S.cm^{-1} at 0.5 wt%, questions the relevance of the costly chemical modification.

Cationic functionalization of GO has been achieved by covalently linking imidazolium to GO. For example, Zhang *et al.* grafted a poly(1,2-diethoxyethylimidazolium) (ox-PIL) (see Fig. 19),[90] and Zhu *et al.* grafted an (3-aminopropyl)-3-methylimidazolium bromide.[92] In both cases LiTFSI is the lithium salt and PEO the polymer matrix (1 10^6 for ref.[92], 6 10^5 for ref.[90]).

Such cationic sites on GO are expected to enhance t_{Li+}, the idea being that the imidazolium moiety will interact/fix the lithium salt anion, decrease its association with Li^+, and lower the activation energy of the Li^+ migration. All these phenomena are expected to reduce/avoid the dendrite growth by improving the ionic conductivity and the t_{Li+}. For these two SPE, a decrease in the T_g as well as the melting temperature T_f of the SPE are observed for a filler content of 1 wt%[92] or 5 wt%.[90] and transport properties: σ at 30 °C = 3.16 x 10^{-5} S.cm^{-1}, $t_{Li+} = 0.61$ for

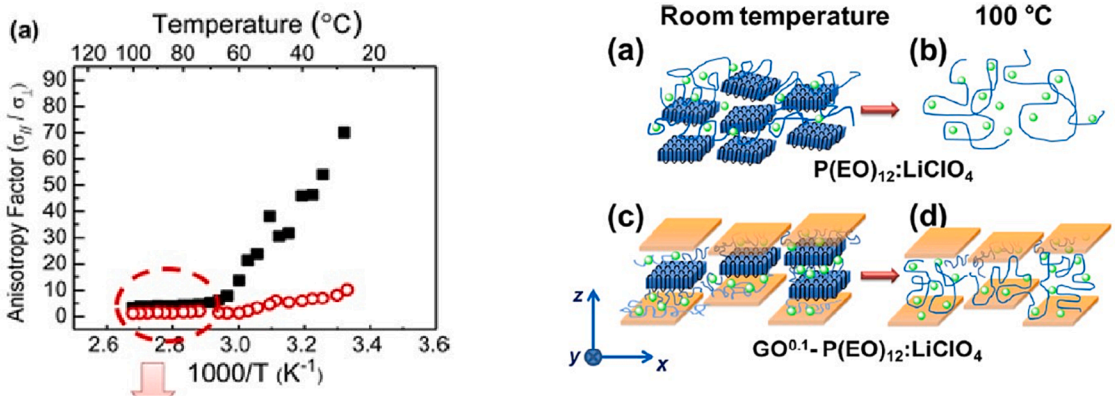

Fig. 18. A/ conductivity anisotropy as a function of temperature calculated from the first heating scan for a P(EO)12:$LiClO_4$ (top) and $GO_{0.1}$-$P(EO)_{12}$:$LiClO_4$ SPE and B/ illustration of the crystalline structure change of such SPE from room temperature (left) to 100 °C (right); reprinted with permission from ref.[74] copyright (2015)

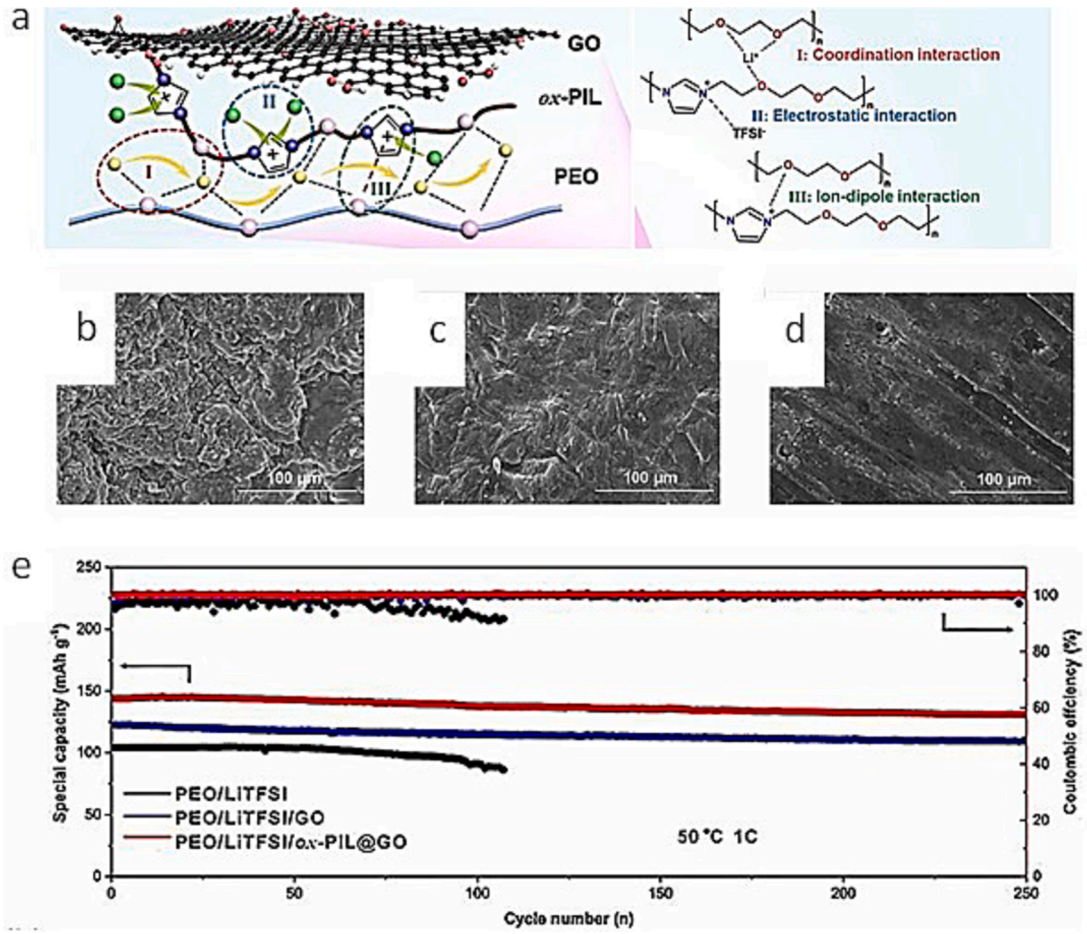

Fig. 19. A/ schematic illustration of the advantages/disadvantages of peo/litfsi, peo/litfsi/go and peo/litfsi/ox-pil@go cpes, b/ sem images of li electrodes after 100 cycles obtained from (b) li|peo/litfsi|li cell, (c) li|peo/litfsi/go|li cell, (d) li|peo/litfsi/ox-pil@go|li cell. e/ battery performance of lfp|cpe|li cells assembled by the peo/litfsi, the peo/litfsi/ go, and the peo/litfsi/ox-pil@go at 1c: (a) at 50 °C; reprinted with permission from ref.[90] copyright (2022)

ref.[92] and σ at 30 °C = 3.16 x 10^{-5} S.cm^{-1} for ref.[90] These values may seem too weak to justify the important cost of preparation for such modified GO, but performance in symmetric cells and in battery with an LFP cathode demonstrate that it is worth it, especially in the case of the ox-PIL SPE. In this case, the discharge capacity was greatly improved: 145 mAh.g^{-1} against 104 mAh.g^{-1} at 0.1C at 50 °C for pristine PEO/LiTFSI and 85 mAh/g at 2C-rate.[90] Besides, the improved electrolyte/electrode interface stability is evidenced by Li stripping/plating experiments showing that with the GO modified with ox-PIL, the PEO/LiTFSI/ox-PIL@GO electrolyte can cycle for more than 800 h without short-circuit compared to 490 h for the PEO/LiTFSI/GO electrolyte.[90] Higher cyclability can be attributed to the limitation of dendrite growth that is corroborated by the smooth, dense and homogeneous surface observed for Li anode and ascribed to the decrease in PEO crystallinity induced by the GO modification.[90].

In both references, the electrolyte/electrode compatibility via the charge/discharge process is demonstrated. In the case of PEO alone, the charge/discharge curves are abrupt and unstable at 1 C. In contrast, by adding GO-IL, the charge/discharge curves are smooth with high coulombic efficiency at 60 °C and 0.1 C.[92,195].

6.4. Unmodified GO in SPE with polymer different from PEO

Besides PEO, PVDF, PVDF-HFP and PMMA-based macromolecules are other polymers reported for SPE elaboration and selected for their physico-chemical properties along with their commercial availability. Here again we differentiate the SPE made with either unmodified or modified GO.[196].

As with PEO, the ionic conductivity is increased by addition of GO for optimal concentration that can be as different as 0.005 wt% for GO/PVDF/$LiClO_4$,[197] 0.8 wt% for GO/PMMA-PPEGMA/LiTFSI,[188] 2.5 wt% for GO/PVDF-HFP,[198] or 9.0 wt% for GO/Chitosan/PMMA/Glycerol.[199] Concentration higher than 10 wt% are generally detrimental, probably because although GO disturbs the crystallisation of the polymer, it is also a non-covalent cross-linker and negatively impacts the mechanical properties at such a high content. The increase in ionic conductivity produced by GO in such polymers is much lower than the one reported in some case for PEO: from + 25 % for GO/PMMA-PPEGMA/LiTFSI,[188] to + 156 % for or 2.5 wt% for GO/PVDF-HFP,[198].

As for PEO, GO also slightly improves the electrical stability (for example up to 4.7 V for PVDF/LiTFSI)[197], t_{Li}+ (up to = 0.74 for PVDF/LiTFSI).[197].

GO also improves the thermal stability of polymers that are generally stable enough at the temperatures envisaged for the operation of the batteries (<120 °C). It also increases the polarity and wettability of polymers like (PVDF- HFP)[198] and polyimide.[200].

In a very recent report, a multicomponent SPE made of Chitosan/GO/PVP/LiTFSI/SiO_2 (100/0.5/10/10/10; ↕0.08 mm) exhibits a σ = 2.76 × 10^{-3} S·cm^{-1} at (23 ∘C), a high t_{Li}+= 0.76 and good cyclability and performance in battery $LiCoO_2$ as cathode. The report underlines the importance of the GO' structure and, although is represent only 1 % of the total mass, a highly porous GO (Holey GO) obtained by an oxidative hydrothermal treatment, multiplies the ionic conductivity by 70

compared with pristine GO.[201].

6.5. Modified GO in SPE with polymers different from PEO for Li-metal battery

In PVDF matrix with $LiClO_4$, sulfonated-GO prepared via diazonium of sulfanilic acid modifies to some extend the mechanical, thermal and structural property even at concentration as low as 0.002, to 0.020 wt%.[202] More significantly, the electrochemical performances obtained for an optimum of 0.004 wt% of GO dramatically increase the transference number ($t_{Li+} = 0.93$), the ionic conductivity (6.2×10^{-3} S cm^{-1} at 40 °C) and the stability (up to 4.7 V vs. Li^+/Li). Performances in Li-$LiMnO_2$ are also clearly improved by the sulfonated-GO. For example, a 55 % increase of energy density was observed (331.5 Wh kg^{-1} without modified GO, 512.0 Wh kg^{-1} with 0.004 wt% of modified GO). Unfortunately, a plating stripping study is not reported. Other reported modifications by anionic functions led to much smaller improvement of the ionic conductivity and obtained with much higher GO concentrations: for an adenosine 5′-diphosphate modified GO σ is 6 time higher (at the best) for 7.5 wt% of GO in PVDF-HFP/LiTFSI (1×10^{-4} S cm^{-1} at 40 °C, $t_{Li}+ = 0.51$).[89].

Example of a GO associated with inorganic solid-state electrolyte are rare, the only example that we found concerns $Li_7P_3S_{11}$ that was coated with GO (0, 0.5, 1.0 and 2.0 wt% in pellets of ↕1mm) for tests in Li//$LiNbO_3$-coated or Li//$LiCoO_2$ batteries. However, the processing at 250 °C for 1 h results in the transformation of GO into rGO and is out of the scope of this review.[203].

6.6. GO in solid-state electrolyte for Zn-O_2 battery

Differently from other batteries, the electrolyte in Zn-O_2 battery is based on fast and continuous shuttling of hydroxide anions. Although O-rich function in GO can performed this through H-bonding of solvated OH^-, GO alone does not exhibit high performances, probably because of the Donnan effect and the size of hydrated OH^- that is too large to enter in the nanochannels d-spacing. To prepare an SPE for Zn-O_2 battery [103] GO and nanocellulose were blended, grafted with ammonium-containing alkoxysilane and cross-linked with glutaraldehyde. The resulting 30–50 μm thick electrolyte offers different pathways for hydroxide mobility either by a Grotthuss type process (direct OH^- jumps from a stationary oxygen atom to a neighbouring oxygen atom after reorientation and correct positioning) or vehicle type process (via translational diffusion phenomenon of the solvated OH^- species).

6.7. GO in solid-state electrolyte for vanadium redox flow battery

For electrolyte of vanadium redox flow batteries (VRFB sometime VFB),[16] the challenge is to permit a fast, massive and selective proton migration without migration of vanadium ions, especially dioxovanadium (VO_2^+) which results in lower battery efficiency and faster capacity fading. Nafion^{TM} membranes are the SPE benchmark in VRB. The limitation of their performances is ascribed to large ion cluster channels causing vanadium ion pathways that result in lower battery efficiency and fast capacity fading. GO has been selected as a potential candidate for improving the performances and assuming strong interfacial interactions with SO_3H-containing polymer. Data of different reports on GO/Nafion^{TM} membrane are summarized in Table 2.

In 2014, Lee *et al.* reported that GO decreases the proton conductivity and the vanadium permeability while increasing the GO content from 0, 0.001, 0.01, 0.1 to 1 wt%.[204] Yong Gun *et al.* also reported such data the same year.[205] But Yu *et al.* then reported improved performance for a GO content of 1.0 wt% that was ascribed mainly to the processing of the membrane that could lead to different level of stacking aggregation of GO.[206] Impressive performance were reported in 2017 for a spin-coated nanolayer of GO/Nafion^{TM} (↕ 400–440 nm, GO content 0.1 or 2 mg g^{-1}) deposited on a re-casted Nafion^{TM} 212 film (↕ 50 μm).[207] In addition to the high performances in battery, the nanofilm with very low GO content increases the tensile strength, decreases the elongation at break, divides by almost 2 the water uptake and divides by 1.5 the swelling ratio.

Graphene oxide also improved the performances of other SO_3H-containing polymer like SPEEK, sulfonated polyimide or mixture of polyvinylpyrrolidone/polysulfone reported in Table 3. SPEEK can clearly compete with Nafion^{TM} and performance can even be slightly improved by amidation of GO with ethylenediamine. However, chemical modification of GO can be disappointing as exemplified by the performance of a highly sophisticated zwitterionic structure of GO bearing poly-(4-vinylbenzyl tetramethylammonium) and poly-(4-vinylbenzenesulfonic) (3.0 at. % of N and 1.8 at.% of S).[97].

From these various works, no general trend emerges concerning the effect of wt.% of GO filler on the membrane properties. Indeed with increasing proportion of GO the proton conductivity increases,[97] decreases[208,209] or passes by an optimum[88] while the permeability to VO_2^+ cation also increases,[88] decreases[208,209] or passes by an optimum.[97] May be related to these observations is that, even at very low content (ca 0.01 wt% of GO), serious agglomeration in SO_3H-containing polymer can occur depending on the processing of the materials.[104].

The effect of GO is even more questionable when comparing it to graphene nanoplate (GNP) as a filler of SPEEK and Nafion^{TM}. For the latter, Yu *et al.* report that GO, compared to G, decreases less the proton conductivity while greatly decreases the VO_2^+ permeability (Table 4).[206] Differently, the two reports by Dai *et al.* on respectively SPEEK/GO [208] and SPEEK/G,[210] data gathered in Table – suggest an opposite situation: G decreases less the proton conductivity and greatly decreases the VO_2^+ permeability compared to GO. This question should be clarified to confirm or infirm the relevance of the usual arguments on the benefit of the O_f onto GO and their role on the migration process of

Table 2
Overview of different data reported on GO/Nafion^{TM} membrane for VRF batteries.

Material	Proton conductivity 10^{-3} S cm^{-1}	Permeability to VO_2^+ 10^{-7} cm^2 min^{-1}	Ionic selectivity 10^7 S min cm^{-3}	CE	VE	EE	Ref.
Nafion 212	76	28	2.7				[207]
GO/Nafion 117 GO-content 0, 0.001, 0.01, 0.1 and 1 wt% thickness 27.8 μm	~35 to ~ 20	~5 to 7	6.3[a]	90 % [a]	90 % [a]	82 %	[204]
GO/Nafion117 GO content: 0 and 1.0 wt% thickness 70 μm	29.3	8	3.7	96		85	[206]
GO/Nafion nanolayer GO content 0.1 or 2 mg g^{-1} thickness 400–440 nm[c]	72	0.82	87.7	96 %[b]	89 %[b]	87.5 %[b]	[207]

CC (Coulombic efficiency), VE (Voltage efficiency) and EE (Energy efficiency) all at 50 mA cm^{-2}.
[a] for GO-content = 0.01 wt%, [b] for GO-content = 2 wt%, [c] on recast Nafion 212 50 μm.

Table 3
Overview of different data reported on GO/SPEEK membranes for VRF batteries.

Material	Proton conductivity 10^{-3} S cm^{-1}	Permeability to VO_2^+ 10^{-7} cm^2 min^{-1}	Ionic selectivity 10^4 S min cm^{-3}	CE	VE	EE	Ref.
GO in SPEEK [a] 1, 2, 3 or 5 wt% of GO 50—60 µm thickness	16.9 to 7, 7	11.5 to 5.2	1.166 to 1.44	~95 %[a]	91 %[a]	87 %[a]	[208]
Ethylenediamine-modified GO in SPEEK[b] GO-content 1, 2, 3, 4, 5 wt% thickness 60 µm	40–50	5 to 10	18.5 to 10	96.5 %[b]	92.4 % [b]	89.2 % [b]	[88]
Zwitterionic-GO in sulfonated polyimide[c] GO-content 0.5, 1, 2, 4, 6 wt% thickness 50 µm	9.2	7.4	0.91	94	79	75	[97]
GO in PSF-PVP[d] GO-content 0.025, 0.05, 0.075, 0.1 wt% Thickness unknown	37 to 22	0.026 to 0,012		95 [d]	80 [d]	75 [d]	[209]
GO with "PTFE" and "commercial perfluorinated sulfonic acid membrane "? GO-content 0.01 wt% thickness 46 µm	9	5.8	4.5	85	95	91	[104]

CC (Coulombic efficiency), VE (Voltage efficiency) and EE (Energy efficiency) all at 50 mA cm^{-2}.
SPEEK sulfonated poly(etheretherketone).
[a] 63 % of SO_3H substitution for SPEEK and performances for 2 wt% of GO, [b] 72 % of SO_3H substitution - GO amidified with ethylenediamine (13.82 % nitrogen) performances for 2 wt% of ethylenediamine-GO, [c] performances for 4 wt% of Zwitterionic-GO, [d] PSF-PVP polyvinylpyrrolidone Polysulfone, (MW 480 000 g mol^{-1})) performance for 0.05 wt%.

Table 4
Comparison of the effect GO and G as a filler of SPEEK and Nafion™.

Materials	Proton conductivity 10^{-3} S cm^{-1}	Permeability 10^{-7} cm^2 min^{-1}	Ref
SPEEK	16.9	11.5	[208]
SPEEK with 1 % GO	15.3 (-10 %)	9.2 (-10 %)	[208]
SPEEEK	15	15.6	[210]
SPEEK with 1 % G	14.1 (-6%)	8.7 (-44 %)	[210]
Nafion 117	31.5	22.5	[206]
Nafion 117 with 1 % GO	29.3 (-5%)	7.5 (-66 %)	[206]
Nafion 117 with 1 % G	26.5 (-16 %)	10.5 (-53 %)	[206]

respectively H^+ and VO_2^+.

7. Conclusion on solid state electrolyte

The above data show that: 1/ the effect of GO for improving ionic conductivity and transference number or to limit the problem of operating batteries like dendrite growth is not demonstrated unambiguously; 2/ beside PEO, other polymers are competitive but may suffer from other limitations (cost, pollution); 3/ when chemical modification of GO is performed, the grafting level is generally not or poorly determined. The true question for such synthetic step is the ratio between its cost and its benefits in terms of performances in batteries; 4/ so far, no clear comparative study shows the advantage of GO over other grafted nanofillers such as metal oxides SiO_2, Al_2O_3 or TiO_2.

7.1. GO as additive of liquid electrolyte

An additive is a chemical compound entering generally in low quantity in a chemical formulation. As part of the progress toward safe Separator/(Liquid electrolyte) system, the additive from the liquid electrolyte reacts initially, at higher potential (in discharge) resulting in the formation of pre-SEI, able to limit the other electrolyte components reaction. Indeed, an improved SEI, preserving from the growth of dendrites is formed. This is among the simplest and most direct solutions and easy to implement on production process. However, the ideal candidate must be cheap, non-toxic, stable and efficient. Liquid electrolytes topic is revisited frequently every year,[211–213] but surprisingly, for "additive"; "electrolyte"; "battery"; "graphene oxide" on Scifinder, results are very limited (49 Journal articles, 19 patents and no review at this time).

A tryptophan-based Graphene oxide as an additive to the electrolyte for aqueous zinc-ion batteries improves their performances (Zn|Zn symmetric battery with 500 h at 0.2 mA cm^{-2} and even more than 250 h at 1.0 mA cm^{-2}). This results in a uniform distribution of the electric field which reduces the nucleation overpotential of Zn metal, provides a more uniform deposition process on the metal surface and improves cyclability of the aqueous Zn-ion battery.[214].

8. Conclusion & perspectives

Graphene oxide is, on the one hand, an attractive material due to its two-dimensional structure, its potentially very high specific surface area and the diversity of its oxygen functions. It is usable in aqueous suspension or in ethanol, can be easily post-modified to adapt it for use in battery electrolyte, and easily processed as a filler with different polymers. On the other hand, it is up to now rather expensive (although cheaper price could be expectable with increasing the capacity), the standardization of its synthesis remains a problem and raises the question of precise structure of the GO used that can deeply vary, modifying the percentages of the different oxygenated functions, the stacking of the nanosheets and their size, the degree of chemical modification when this is carried out, *etc.* all of which impact the performance in applications.

This being said, the various examples that we have reported in this review show that chemists have proven that GO has a strong potential to increase the lifespan of new generation batteries, particularly those with a metal anode (Li, but not only). Given its mechanical and structural properties, it has been widely and successfully explored to limit polysulfide shuttling and dendrite growth. However, other physicochemical properties deserve to be studied in the light of recent progresses on the parameters which control the formation and properties of the SEI, in particular surface energy. Almost all possible combinations of use of GO have been explored, including its association with a commercial separator, the synthesis of new separators, or the protection of the electrodes by surface films. However, the comparison of electrochemical performances is currently not always relevant (or at least challenging), since so

many different experimental conditions are used: nature and composition of the electrodes and electrolyte, temperature… From this point of view, the scientific community should move toward standardized assays. Besides, too frequently experimental information is missing in reports such as technical data of the reagents (purity, molecular weight of polymer), experimental parameters (T°, pH, concentration, time), characteristics of the SPE (composition and proportion, thickness, fiber diameters) and electrochemical test conditions.

Finally, in the context of the use of GO as part of the electrolyte in batteries, more fundamental and modelling studies seem essential to carry out. Without being exhaustive, we believe the next point to be taken into account: the ionic conductivity of pure GO according to the synthesis conditions; the GO/salt and GO/solvent interaction (in particular the ionic liquids and carbonates, commonly used); the electrochemical oxidation of GO in battery, to understand its evolution at the interface with the electrodes; and last but not least, the GO/polymer interaction, that is determinant for SPE and that can evolve upon cycling.

Funding

This work was supported by the "Chimie Balard CIRIMAT Carnot Institute" through the ANR program N°16 CARN 0008–01.

CRediT authorship contribution statement

Charlotte Maignan: Data curation, Formal analysis, Writing – original draft, Writing – review & editing. **Johan G. Alauzun:** Formal analysis, Writing – original draft, Writing – review & editing. **Emmanuel Flahaut:** Funding acquisition, Writing – original draft, Writing – review & editing. **Laure Monconduit:** Formal analysis, Funding acquisition, Supervision, Writing – original draft, Writing – review & editing. **Bruno Boury:** Conceptualization, Data curation, Visualization, Writing – original draft, Writing – review & editing.

Declaration of competing interest

The authors declare that they have no known competing financial interests or personal relationships that could have appeared to influence the work reported in this paper.

Data availability

No data was used for the research described in the article.

References

[1] D. Lin, Y. Liu, Y. Cui, Reviving the lithium metal anode for high-energy batteries, Nat. Nanotechnol. 12 (3) (2017) 194–206.
[2] M. Armand, Polymer solid electrolytes - an overview, Solid State Ion 9–10 (1983) 745–754.
[3] M. Armand, J. Chabagno, M. Duclot. (1978). Polymeric solid electrolytes. *The 2nd International conference on solid electrolyte. Ext. Abs., St. Andrews, Scotland, 1978.* (Vol. 2309, pp. 6-5).
[4] F. Li, X. Jiang, J. Zhao, S. Zhang, Graphene oxide: A promising nanomaterial for energy and environmental applications, Nano Energy 16 (2015) 488–515.
[5] A. Eftekhari, Y.M. Shulga, S.A. Baskakov, G.L. Gutsev, Graphene oxide membranes for electrochemical energy storage and conversion, Int. J. Hydrogen Energy 43 (4) (2018) 2307–2326.
[6] Y. Tian, Z. Yu, L. Cao, X.L. Zhang, C. Sun, D.-W. Wang, Graphene oxide emerging electromaterial for energy storage and conversion, J. Energy Chem. 55 (2021) 323–344.
[7] S. Gahlot, V. Kulshrestha, Graphene based polymer electrolyte membranes for electro-chemical energy applications, Int. J. Hydrogen Energy 45 (34) (2020) 17029–17056.
[8] D. Dhamodharan, P.P. Ghoderao, V. Dhinakaran, S. Mubarak, N. Divakaran, H.-S. Byun, A review on graphene oxide effect in energy storage devices, J. Ind. Eng. Chem. 106 (2022) 20–36.
[9] W. Liu, P. Liu, D. Mitlin, Tutorial review on structure - dendrite growth relations in metal battery anode supports, Chem. Soc. Rev. 49 (20) (2020) 7284–7300.
[10] Z. Tong, S.-B. Wang, Y.-K. Liao, S.-F. Hu, R.-S. Liu, Interface Between Solid-State Electrolytes and Li-Metal Anodes: Issues, Materials, and Processing Routes, ACS Appl. Mater. Interfaces 12 (42) (2020) 47181–47196.
[11] S. Gao, F. Sun, N. Liu, H. Yang, P.-F. Cao, Ionic conductive polymers as artificial solid electrolyte interphase films in Li metal batteries – A review, Mater. Today 40 (2020) 140–159.
[12] X. Miao, S. Guan, C. Ma, L. Li, C.-W. Nan, Role of Interfaces in Solid-State Batteries, *Adv. Mater.*, n/a(n/a), 2206402.
[13] X. Gao, Y.-N. Zhou, D. Han, J. Zhou, D. Zhou, W. Tang, J.B. Goodenough, Thermodynamic Understanding of Li-Dendrite Formation, Joule 4 (9) (2020) 1864–1879.
[14] L. Su, A. Manthiram, Lithium-Metal Batteries via Suppressing Li Dendrite Growth and Improving Coulombic Efficiency, Small Structures 3 (10) (2022) 2200114.
[15] J.N. Chazalviel, Electrochemical aspects of the generation of ramified metallic electrodeposits, Phys. Rev. A 42 (12) (1990) 7355–7367.
[16] Z. Yuan, H. Zhang, X. Li, Ion conducting membranes for aqueous flow battery systems, Chem. Commun. 54 (55) (2018) 7570–7588.
[17] A. Eftekhari, LiFePO4/C nanocomposites for lithium-ion batteries, J. Power Sources 343 (2017) 395–411.
[18] J. Lu, Z. Chen, Z. Ma, F. Pan, L.A. Curtiss, K. Amine, The role of nanotechnology in the development of battery materials for electric vehicles, Nat. Nanotechnol. 11 (12) (2016) 1031–1038.
[19] P. Roy, S.K. Srivastava, Nanostructured anode materials for lithium ion batteries, J. Mater. Chem. A 3 (6) (2015) 2454–2484.
[20] D.C. Marcano, D.V. Kosynkin, J.M. Berlin, A. Sinitskii, Z. Sun, A. Slesarev, J. M. Tour, Improved Synthesis of Graphene Oxide, ACS Nano 4 (8) (2010) 4806–4814.
[21] W.S. Hummers Jr., R.E. Offeman, Preparation of Graphitic Oxide, J. Am. Chem. Soc. 80 (6) (1958) 1339.
[22] S. Stankovich, D.A. Dikin, R.D. Piner, K.A. Kohlhaas, A. Kleinhammes, Y. Jia, R. S. Ruoff, Synthesis of graphene-based nanosheets via chemical reduction of exfoliated graphite oxide, Carbon 45 (7) (2007) 1558–1565.
[23] R.K. Singh, R. Kumar, D.P. Singh, Graphene oxide: strategies for synthesis, reduction and frontier applications, RSC Adv. 6 (69) (2016) 64993–65011.
[24] Y.-M. Chen, S.-T. Hsu, Y.-H. Tseng, T.-F. Yeh, S.-S. Hou, J.-S. Jan, H. Teng, Minimization of ion-solvent clusters in gel electrolytes containing graphene oxide quantum dots for lithium-ion batteries, Small 14 (12) (2018) n/a.
[25] S. Valizadeh, L. Naji, M. Karimi, S. Sarabadani Tafreshi, B. Heijman, N.H. de Leeuw, Experimental and density functional theory studies of laminar double-oxidized graphene oxide nanofiltration membranes, Chem. Eng. Res. Des. 188 (2022) 590–606.
[26] L.P. Bakos, M. Bohus, I.M. Szilágyi, Investigating the Reduction/Oxidation Reversibility of Graphene Oxide for Photocatalytic Applications, Molecule 28 (11) (2023) 4344.
[27] C.A. Zito, T.M. Perfecto, T. Mazon, A.-C. Dippel, D. Koziej, D.P. Volanti, Reoxidation of graphene oxide: Impact on the structure, chemical composition, morphology and dye adsorption properties, Appl. Surf. Sci. 567 (2021) 150774.
[28] D. Chen, H. Feng, J. Li, Graphene Oxide: Preparation, Functionalization, and Electrochemical Applications, Chem. Rev. 112 (11) (2012) 6027–6053.
[29] R.L.D. Whitby, Chemical Control of Graphene Architecture: Tailoring Shape and Properties, ACS Nano 8 (10) (2014) 9733–9754.
[30] R. Cruz-Silva, M. Endo, M. Terrones, Graphene oxide films, fibers, and membranes, Nanotechnol. Rev. 5 (4) (2016) 377–391.
[31] S. Ye, J. Feng, The effect of sonication treatment of graphene oxide on the mechanical properties of the assembled films, RSC Adv. 6 (46) (2016) 39681–39687.
[32] W. Du, H. Wu, H. Chen, G. Xu, C. Li, Graphene oxide in aqueous and nonaqueous media: Dispersion behaviour and solution chemistry, Carbon 158 (2020) 568–579.
[33] S.H. Aboutalebi, M.M. Gudarzi, Q.B. Zheng, J.-K. Kim, Spontaneous Formation of Liquid Crystals in Ultralarge Graphene Oxide Dispersions, Adv. Funct. Mater. 21 (15) (2011) 2978–2988.
[34] Z. Xu, C. Gao, Aqueous Liquid Crystals of Graphene Oxide, ACS Nano 5 (4) (2011) 2908–2915.
[35] J.E. Kim, T.H. Han, S.H. Lee, J.Y. Kim, C.W. Ahn, J.M. Yun, S.O. Kim, G.O. L. Crystals, Angew. Chem., Int. Ed. 50 (13) (2011) 3043–3047.
[36] Q. Pan, C.-C. Chung, N. He, J.L. Jones, W. Gao, Accelerated Thermal Decomposition of Graphene Oxide Films in Air via in Situ X-ray Diffraction Analysis, J. Phys. Chem. C 120 (27) (2016) 14984–14990.
[37] D.A. Dikin, S. Stankovich, E.J. Zimney, R.D. Piner, G.H.B. Dommett, G. Evmenenko, R.S. Ruoff, Preparation and characterization of graphene oxide paper, Nature 448 (7152) (2007) 457–460.
[38] S. Naficy, R. Jalili, S.H. Aboutalebi, R.A. Gorkin Iii, K. Konstantinov, P.C. Innis, G. G. Wallace, Graphene oxide dispersions: tuning rheology to enable fabrication, Mater. Horiz. 1 (3) (2014) 326–331.
[39] K. Fu, Y. Yao, J. Dai, L. Hu, Progress in 3D Printing of Carbon Materials for Energy-Related Applications, Adv. Mater. 29 (9) (2017) n/a.
[40] D. Wei, X. Liu, S. Lv, L. Liu, L. Wu, Z. Li, Y. Hou, Fabrication, Structure, Performance, and Application of Graphene-Based Composite Aerogel, Materials 15 (1) (2022) 299.
[41] Y. Chen, X. Su, D. Esmail, E. Buck, S.D. Tran, T. Szkopek, M. Cerruti, Dual-templating strategy for the fabrication of graphene oxide, reduced graphene oxide and composite scaffolds with hierarchical architectures, Carbon 189 (2022) 186–198.

[42] H. Huang, H. Shi, P. Das, J. Qin, Y. Li, X. Wang, H.-M. Cheng, The Chemistry and Promising Applications of Graphene and Porous Graphene Materials, Adv. Funct. Mater. 30 (41) (2020) 1909035.

[43] R.K. Joshi, P. Carbone, F.C. Wang, V.G. Kravets, Y. Su, I.V. Grigorieva, R.R. Nair, Precise and Ultrafast Molecular Sieving Through Graphene Oxide Membranes, Science 343 (6172) (2014) 752–754.

[44] P. Sun, K. Wang, H. Zhu, Recent Developments in Graphene-Based Membranes: Structure, Mass-Transport Mechanism and Potential Applications, Adv. Mater. 28 (12) (2016) 2287–2310.

[45] P. Su, F. Wang, Z. Li, C.Y. Tang, W. Li, Graphene oxide membranes: controlling their transport pathways, J. Mater. Chem. A 8 (31) (2020) 15319–15340.

[46] A. Ali, M. Aamir, K.H. Thebo, J. Akhtar, Laminar Graphene Oxide Membranes Towards Selective Ionic and Molecular Separations: Challenges and Progress, Chem. Rec. 20 (4) (2020) 344–354.

[47] S.D. Lacey, D.J. Kirsch, Y. Li, J.T. Morgenstern, B.C. Zarket, Y. Yao, L. Hu, Extrusion-Based 3D Printing of Hierarchically Porous Advanced Battery Electrodes, Adv. Mater. 30 (12) (2018) n/a.

[48] H. Zhang, Q. He, J. Luo, Y. Wan, S.B. Darling, Sharpening Nanofiltration: Strategies for Enhanced Membrane Selectivity, ACS Appl. Mater. Interfaces 12 (36) (2020) 39948–39966.

[49] L. Ji, M. Rao, H. Zheng, L. Zhang, Y. Li, W. Duan, Y. Zhang, Graphene Oxide as a Sulfur Immobilizer in High Performance Lithium/Sulfur Cells, J. Am. Chem. Soc. 133 (46) (2011) 18522–18525.

[50] S.C. Park, T.H. Lee, G.H. Moon, B.S. Kim, J.M. Roh, Y.H. Cho, Y.S. Kang, Sub-5 nm Graphene Oxide Nanofilm with Exceptionally High H+/V Selectivity for Vanadium Redox Flow Battery, ACS Appl. Energy Mater. 2 (7) (2019) 4590–4596.

[51] A. Ganguly, S. Sharma, P. Papakonstantinou, J. Hamilton, Probing the Thermal Deoxygenation of Graphene Oxide Using High-Resolution In Situ X-ray-Based Spectroscopies, J. Phys. Chem. C 115 (34) (2011) 17009–17019.

[52] M. Acik, G. Lee, C. Mattevi, A. Pirkle, R.M. Wallace, M. Chhowalla, Y. Chabal, The Role of Oxygen during Thermal Reduction of Graphene Oxide Studied by Infrared Absorption Spectroscopy, J. Phys. Chem. C 115 (40) (2011) 19761–19781.

[53] Y. Qiu, F. Guo, R. Hurt, I. Külaots, Explosive thermal reduction of graphene oxide-based materials: Mechanism and safety implications, Carbon 72 (2014) 215–223.

[54] M. Pumera, Electrochemistry of graphene, graphene oxide and other graphenoids: Review, Electrochem. Commun. 36 (2013) 14–18.

[55] A. Ambrosi, A. Bonanni, Z. Sofer, J.S. Cross, M. Pumera, Electrochemistry at Chemically Modified Graphenes, Chem. Eur. J. 17 (38) (2011) 10763–10770.

[56] M. Zhou, Y. Wang, Y. Zhai, J. Zhai, W. Ren, F. Wang, S. Dong, Controlled Synthesis of Large-Area and Patterned Electrochemically Reduced Graphene Oxide Films, Chem. Eur. J. 15 (25) (2009) 6116–6120.

[57] S.J. An, Y. Zhu, S.H. Lee, M.D. Stoller, T. Emilsson, S. Park, R.S. Ruoff, Thin Film Fabrication and Simultaneous Anodic Reduction of Deposited Graphene Oxide Platelets by Electrophoretic Deposition, J. Phys. Chem. Lett. 1 (8) (2010) 1259–1263.

[58] H.-L. Guo, X.-F. Wang, Q.-Y. Qian, F.-B. Wang, X.-H. Xia, A Green Approach to the Synthesis of Graphene Nanosheets, ACS Nano 3 (9) (2009) 2653–2659.

[59] A. Ambrosi, M. Pumera, Precise Tuning of Surface Composition and Electron-Transfer Properties of Graphene Oxide Films through Electroreduction, Chem. Eur. J. 19 (15) (2013) 4748–4753.

[60] L.-K. Zhang, H.-M. Xu, M.-X. Jing, L.-X. Li, H. Yang, X.-Q. Shen, Solid Electrolyte/Lithium Anodes Stabilized by Reduced Graphene Oxide Interlayers: Implications for Solid-State Lithium Batteries, ACS Appl. Nano Mater. 4 (9) (2021) 9471–9478.

[61] Y. Yang, L. Ai, S. Yu, J. He, T. Xu, D. Chen, L. Shen, 3D-Printed Porous GO Framework Enabling Dendrite-Free Lithium-Metal Anodes, ACS Appl. Energy Mater. 5 (12) (2022) 15666–15672.

[62] S. Li, X.-S. Wang, Q.-D. Li, Q. Liu, P.-R. Shi, J. Yu, Q.-H. Yang, A multifunctional artificial protective layer for producing an ultra-stable lithium metal anode in a commercial carbonate electrolyte, J. Mater. Chem. A 9 (12) (2021) 7667–7674.

[63] M. Ye, J. Gao, Y. Xiao, T. Xu, Y. Zhao, L. Qu, Metal/graphene oxide batteries, Carbon 125 (2017) 299–307.

[64] M. Ye, Y. Xiao, Z. Cheng, L. Cui, L. Jiang, L. Qu, A smart, anti-piercing and eliminating-dendrite lithium metal battery, Nano Energy 49 (2018) 403–410.

[65] G. Zhao, J. Li, L. Jiang, H. Dong, X. Wang, W. Hu, Synthesizing MnO2 nanosheets from graphene oxide templates for high performance pseudosupercapacitors, Chem. Sci. 3 (2) (2012) 433–437.

[66] B. Xu, S. Yue, Z. Sui, X. Zhang, S. Hou, G. Cao, Y. Yang, What is the choice for supercapacitors: graphene or graphene oxide? Energy Environ. Sci. 4 (8) (2011) 2826–2830.

[67] P. Zhou, X. Zhang, Y. Xiang, K. Liu, Strategies to enhance Li+ transference number in liquid electrolytes for better lithium batteries, Nano. Res. (2022).

[68] M.R. Karim, K. Hatakeyama, T. Matsui, H. Takehira, T. Taniguchi, M. Koinuma, S. Hayami, Graphene Oxide Nanosheet with High Proton Conductivity, J. Am. Chem. Soc. 135 (22) (2013) 8097–8100.

[69] K. Hatakeyama, M.R. Karim, C. Ogata, H. Tateishi, A. Funatsu, T. Taniguchi, Y. Matsumoto, Proton Conductivities of Graphene Oxide Nanosheets: Single, Multilayer, and Modified Nanosheets, Angew. Chem., Int. Ed. 53 (27) (2014) 6997–7000.

[70] W. Gao, G. Wu, M.T. Janicke, D.A. Cullen, R. Mukundan, J.K. Baldwin, P. Zelenay, Ozonated Graphene Oxide Film as a Proton-Exchange Membrane, Angew. Chem., Int. Ed. 53 (14) (2014) 3588–3593.

[71] H. Tateishi, T. Koga, K. Hatakeyama, A. Funatsu, M. Koinuma, T. Taniguchi, Y. Matsumoto, Graphene oxide lead battery (GOLB), ECS Electrochem. Lett. 3 (3) (2014) A19.

[72] A.A. Azli, N.S.A. Manan, M.F.Z. Kadir, The development of Li+ conducting polymer electrolyte based on potato starch/graphene oxide blend, Ionics 23 (2) (2017) 411–425.

[73] H. Liao, H. Zhang, G. Qin, Z. Li, L. Li, H. Hong, A macro-porous graphene oxide-based membrane as a separator with enhanced thermal stability for high-safety lithium-ion batteries, RSC Adv. 7 (36) (2017) 22112–22120.

[74] S. Cheng, D.M. Smith, C.Y. Li, Anisotropic Ion Transport in a Poly(ethylene oxide)-LiClO4 Solid State Electrolyte Templated by Graphene Oxide, Macromolecules 48 (13) (2015) 4503–4510.

[75] K.M. Diederichsen, E.J. McShane, B.D. McCloskey, Promising Routes to a High Li + Transference Number Electrolyte for Lithium Ion Batteries, ACS Energy Lett 2 (11) (2017) 2563–2575.

[76] P. Barai, K. Higa, V. Srinivasan, Impact of External Pressure and Electrolyte Transport Properties on Lithium Dendrite Growth, J. Electrochem. Soc. 165 (11) (2018) A2654.

[77] T. Foroozan, F.A. Soto, V. Yurkiv, S. Sharifi-Asl, R. Deivanayagam, Z. Huang, R. Shahbazian-Yassar, Synergistic Effect of Graphene Oxide for Impeding the Dendritic Plating of Li, Adv. Funct. Mater. 28 (15) (2018) n/a.

[78] H. Shi, J. Qin, K. Huang, P. Lu, C. Zhang, Y. Dong, Z.-S. Wu, A Two-Dimensional Mesoporous Polypyrrole-Graphene Oxide Heterostructure as a Dual-Functional Ion Redistributor for Dendrite-Free Lithium Metal Anodes, Angew. Chem., Int. Ed. 59 (29) (2020) 12147–12153.

[79] J. Cao, D. Zhang, X. Zhang, M. Sawangphruk, J. Qin, R. Liu, A universal and facile approach to suppress dendrite formation for a Zn and Li metal anode, J. Mater. Chem. A 8 (18) (2020) 9331–9344.

[80] S. Guo, S. Garaj, A. Bianco, C. Ménard-Moyon, Controlling covalent chemistry on graphene oxide, Nat. Rev. Phys. 4 (4) (2022) 247–262.

[81] V. Georgakilas, J.N. Tiwari, K.C. Kemp, J.A. Perman, A.B. Bourlinos, K.S. Kim, R. Zboril, Noncovalent Functionalization of Graphene and Graphene Oxide for Energy Materials, Biosensing, Catalytic, and Biomedical Applications, Chem. Rev. 116 (9) (2016) 5464–5519.

[82] Y.Y. Khine, X. Wen, X. Jin, T. Foller, R. Joshi, Functional groups in graphene oxide, Phys. Chem. Chem. Phys. 24 (43) (2022) 26337–26355.

[83] C. Zhang, Y. Lin, Y. Zhu, Z. Zhang, J. Liu, Improved lithium-ion and electrically conductive sulfur cathode for all-solid-state lithium-sulfur batteries, RSC Adv. 7 (31) (2017) 19231–19236.

[84] J. Shim, D.-G. Kim, H.J. Kim, J.H. Lee, J.-H. Baik, J.-C. Lee, Novel composite polymer electrolytes containing poly(ethylene glycol)-grafted graphene oxide for all-solid-state lithium-ion battery applications, J. Mater. Chem. A 2 (34) (2014) 13873–13883.

[85] W. Li, Z. Zhu, W. Shen, J. Tang, G. Yang, Z. Xu, A novel PVdF-based composite gel polymer electrolyte doped with ionomer modified graphene oxide, RSC Adv. 6 (99) (2016) 97338–97345.

[86] P. Polrolniczak, M. Walkowiak, J. Kazmierczak-Razna, D. Kasprzak, D.E. Mathew, M. Kathiresan, N. Angulakshmi, BaTiO3-g-GO as an efficient permselective material for lithium-sulfur batteries, Mater. Chem. Front. 5 (2) (2021) 950–960.

[87] N. Angulakshmi, G.P. Kar, S. Bose, E.B. Gowd, S. Thomas, A.M. Stephan, A high-performance BaTiO3-grafted-GO-laden poly(ethylene oxide)-based membrane as an electrolyte for all-solid lithium-batteries, Mater. Chem. Front. 1 (2) (2017) 269–277.

[88] S. Liu, D. Li, L. Wang, H. Yang, X. Han, B. Liu, Ethylenediamine-functionalized graphene oxide incorporated acid-base ion exchange membranes for vanadium redox flow battery, Electrochim. Acta 230 (2017) 204–211.

[89] J. Liang, W. Deng, X. Zhou, S. Liang, Z. Hu, B. He, Z. Liu, High Li-Ion Conductivity Artificial Interface Enabled by Li-Grafted Graphene Oxide for Stable Li Metal Pouch Cell, ACS Appl. Mater. Interfaces 13 (25) (2021) 29500–29510.

[90] W. Bao, Z. Hu, Y. Wang, J. Jiang, S. Huo, W. Fan, Y. Zhang, Poly(ionic liquid)-functionalized graphene oxide towards ambient temperature operation of all-solid-state PEO-based polymer electrolyte lithium metal batteries, *Chem. Eng. J.*, 437(Part_1), (2022) 135420.

[91] B. Lin, H. Shang, F. Chu, Y. Ren, N. Yuan, B. Jia, J. Ding, Ionic liquid-tethered Graphene Oxide/Ionic Liquid Electrolytes for Highly Efficient Dye Sensitized Solar Cells, Electrochim. Acta 134 (2014) 209–214.

[92] Z. Hu, X. Zhang, J. Liu, Y. Zhu, Ion Liquid Modified GO Filler to Improve the Performance of Polymer Electrolytes for Li Metal Batteries, Front. Chem. 8 (2020) 00232.

[93] I. Nicotera, C. Simari, M. Agostini, A. Enotiadis, S. Brutti, A Novel Li+-Nafion-Sulfonated Graphene Oxide Membrane as Single Lithium-Ion Conducting Polymer Electrolyte for Lithium Batteries, J. Phys. Chem. C 123 (45) (2019) 27406–27416.

[94] A. Enotiadis, K. Angjeli, N. Baldino, I. Nicotera, D. Gournis, Graphene-Based Nafion Nanocomposite Membranes: Enhanced Proton Transport and Water Retention by Novel Organo-functionalized Graphene Oxide Nanosheets, Small 8 (21) (2012) 3338–3349.

[95] M. Hamrahjoo, S. Hadad, E. Dehghani, M. Salami-Kalajahi, H. Roghani-Mamaqani, Preparation of matrix-grafted graphene/poly(poly(ethylene glycol) methyl ether methacrylate) nanocomposite gel polymer electrolytes by reversible addition-fragmentation chain transfer polymerization for lithium ion batteries, Eur. Polym. J. 176 (2022) 111419.

[96] L. Ma, X. Yang, L. Gao, M. Lu, C. Guo, Y. Li, X. Zhu, Synthesis and characterization of polymer grafted graphene oxide sheets using a Ce(IV)/HNO3 redox system in an aqueous solution, Carbon 53 (2013) 269–276.

[97] L. Cao, L. Kong, L. Kong, X. Zhang, H. Shi, Novel sulfonated polyimide/zwitterionic polymer-functionalized graphene oxide hybrid membranes for vanadium redox flow battery, J. Power Sources 299 (2015) 255–264.

[98] C. Li, S. Liu, C. Shi, G. Liang, Z. Lu, R. Fu, D. Wu, Two-dimensional molecular brush-functionalized porous bilayer composite separators toward ultrastable high-current density lithium metal anodes, Nat. Commun. 10 (1) (2019) 1363.
[99] S. Agnello, A. Alessi, G. Buscarino, A. Piazza, A. Maio, L. Botta, R. Scaffaro, Structural and thermal stability of graphene oxide-silica nanoparticles nanocomposites, J. Alloys Compd. 695 (2017) 2054–2064.
[100] A. Maio, S. Agnello, R. Khatibi, L. Botta, A. Alessi, A. Piazza, R. Scaffaro, A rapid and eco-friendly route to synthesize graphene-doped silica nanohybrids, J. Alloys Compd. 664 (2016) 428–438.
[101] Z. Luo, G. Zhu, L. Yin, F. Li, B.B. Xu, L. Dala, K. Luo, A Facile Surface Preservation Strategy for the Lithium Anode for High-Performance Li–O2 Batteries, ACS Appl. Mater. Interfaces 12 (24) (2020) 27316–27326.
[102] W.L. Zhang, H.J. Choi, Silica-Graphene Oxide Hybrid Composite Particles and Their Electroresponsive Characteristics, Langmuir 28 (17) (2012) 7055–7062.
[103] J. Zhang, J. Fu, X. Song, G. Jiang, H. Zarrin, P. Xu, Z. Chen, Laminated Cross-Linked Nanocellulose/Graphene Oxide Electrolyte for Flexible Rechargeable Zinc-Air Batteries, Adv. Energy Mater. 6 (14) (2016) 1600476.
[104] J. Ye, C. Zheng, J. Liu, T. Sun, S. Yu, H. Li, In Situ Grown Tungsten Trioxide Nanoparticles on Graphene Oxide Nanosheet to Regulate Ion Selectivity of Membrane for High Performance Vanadium Redox Flow Battery, Adv. Funct. Mater. 32 (8) (2022) 2109427.
[105] B. Boateng, X. Zhang, C. Zhen, D. Chen, Y. Han, C. Feng, W. He, Recent advances in separator engineering for effective dendrite suppression of Li-metal anodes, Nano Select 2 (6) (2021) 993–1010.
[106] S. Ponnada, M.S. Kiai, D.B. Gorle, S. Rajagopal, S. Andra, A. Nowduri, K. Muniasamy, Insight into Lithium-Sulfur Batteries with Novel Modified Separators: Recent Progress and Perspectives, Energy & Fuels 35 (14) (2021) 11089–11117.
[107] H. Hao, T. Hutter, B.L. Boyce, J. Watt, P. Liu, D. Mitlin, Review of Multifunctional Separators: Stabilizing the Cathode and the Anode for Alkali (Li, Na, and K) Metal-Sulfur and Selenium Batteries, Chem. Rev. 122 (9) (2022) 8053–8125.
[108] J. Zhu, M. Yanilmaz, K. Fu, C. Chen, Y. Lu, Y. Ge, X. Zhang, Understanding glass fiber membrane used as a novel separator for lithium–sulfur batteries, J. Membr. Sci. 504 (2016) 89–96.
[109] J.-Q. Huang, T.-Z. Zhuang, Q. Zhang, H.-J. Peng, C.-M. Chen, F. Wei, Permselective Graphene Oxide Membrane for Highly Stable and Anti-Self-Discharge Lithium-Sulfur Batteries, ACS Nano 9 (3) (2015) 3002–3011.
[110] A. Terella, F. De Giorgio, M. Rahmanipour, L. Malavolta, E. Paolasini, D. Fabiani, C. Arbizzani, Functional separators for the batteries of the future, J. Power Sources 449 (2020) 227556.
[111] T.-Z. Zhuang, J.-Q. Huang, H.-J. Peng, L.-Y. He, X.-B. Cheng, C.-M. Chen, Q. Zhang, Rational Integration of Polypropylene/Graphene Oxide/Nafion as Ternary-Layered Separator to Retard the Shuttle of Polysulfides for Lithium-Sulfur Batteries, Small 12 (3) (2016) 381–389.
[112] Y. Zhang, L. Miao, J. Ning, Z. Xiao, L. Hao, B. Wang, L. Zhi, A graphene-oxide-based thin coating on the separator: an efficient barrier towards high-stable lithium–sulfur batteries, 2D Materials 2 (2) (2015) 024013.
[113] C. Shen, Y. Li, M. Gong, C. Zhou, Q. An, X. Xu, L. Mai, Ultrathin Cobalt Phthalocyanine@Graphene Oxide Layer-Modified Separator for Stable Lithium-Sulfur Batteries, ACS Appl. Mater. Interfaces 13 (50) (2021) 60046–60053.
[114] D. Dai, Y. Chen, B. Chen, J. Qiu, B. Li, B. Wang, Nano cellulose fibers and graphene oxide coating on polyolefin separator with uniform Li+ transportation channels for long-life and high-safety Li metal battery, J. Electrochem. Energy Convers. Storage 19 (1) (2022) 010901.
[115] J. Cui, Z. Li, J. Li, S. Li, J. Liu, M. Shao, M. Wei, An atomic-confined-space separator for high performance lithium-sulfur batteries, J. Mater. Chem. A 8 (4) (2020) 1896–1903.
[116] Y. Pan, J. Hao, X. Zhu, Y. Zhou, S.-L. Chou, Ion selective separators based on graphene oxide for stabilizing lithium organic batteries, Inorg. Chem. Front. 5 (8) (2018) 1869–1875.
[117] G. Jiang, K. Li, J. Mao, N. Jiang, J. Luo, G. Ding, Y. Li, Sandwich-like Prussian blue/graphene oxide composite films as ion-sieves for fast and uniform Li ionic flux in highly stable Li metal batteries, Chem. Eng. J. 385 (2020) 123398.
[118] C. Fang, Z. Ye, Y. Wang, X. Zhao, Y. Huang, R. Zhao, Y. Huang, Immobilizing an organic electrode material through π-π interaction for high-performance Li-organic batteries, J. Mater. Chem. A 7 (39) (2019) 22398–22404.
[119] Y. Choi, K. Zhang, K.Y. Chung, D.H. Wang, J.H. Park, PVdF-HFP/exfoliated graphene oxide nanosheet hybrid separators for thermally stable Li-ion batteries, RSC Adv. 6 (84) (2016) 80706–80711.
[120] G. Zhu, X. Jing, D. Chen, W. He, Novel composite separator for high power density lithium-ion battery, Int. J. Hydrogen Energy 45 (4) (2020) 2917–2924.
[121] Y. Chen, J. Li, Y. Ju, R. Cheng, Y. Zhai, J. Sheng, L. Li, Regulating Li-ion flux distribution via holey graphene oxide functionalized separator for dendrite-inhibited lithium metal battery, Appl. Surf. Sci. 592 (2022) 153222.
[122] L.-L. Zuo, Q. Ma, S.-C. Li, B.-C. Lin, M. Fan, Q.-H. Meng, X.-X. Zeng, Highly Thermal Conductive Separator with In-Built Phosphorus Stabilizer for Superior Ni-Rich Cathode Based Lithium Metal Batteries, Adv. Energy Mater. 11 (3) (2021) 2003285.
[123] S.N. Banitaba, D. Semnani, E. Heydari-Soureshjani, B. Rezaei, A.A. Ensafi, Nanofibrous poly(ethylene oxide)-based structures incorporated with multi-walled carbon nanotube and graphene oxide as all-solid-state electrolytes for lithium ion batteries, Polym. Int. 68 (10) (2019) 1787–1794.
[124] K. Khassi, M. Youssefi, D. Semnani, PVDF/TiO2/graphene oxide composite nanofiber membranes serving as separators in lithium-ion batteries, J. Appl. Polym. Sci. 137 (23) (2020) 48775.
[125] P. Zhu, J. Zhu, J. Zang, C. Chen, Y. Lu, M. Jiang, X. Zhang, A novel bi-functional double-layer rGO–PVDF/PVDF composite nanofiber membrane separator with enhanced thermal stability and effective polysulfide inhibition for high-performance lithium–sulfur batteries, J. Mater. Chem. A 5 (29) (2017) 15096–15104.
[126] T. Tatsuma, M. Taguchi, M. Iwaku, T. Sotomura, N. Oyama, Inhibition effects of polyacrylonitrile gel electrolytes on lithium dendrite formation, J. Electroanal. Chem. 472 (2) (1999) 142–146.
[127] A.I. Gopalan, P. Santhosh, K.M. Manesh, J.H. Nho, S.H. Kim, C.-G. Hwang, K.-P. Lee, Development of electrospun PVdF–PAN membrane-based polymer electrolytes for lithium batteries, J. Membr. Sci. 325 (2) (2008) 683–690.
[128] J. Zhu, C. Chen, Y. Lu, J. Zang, M. Jiang, D. Kim, X. Zhang, Highly porous polyacrylonitrile/graphene oxide membrane separator exhibiting excellent anti-self-discharge feature for high-performance lithium-sulfur batteries, Carbon 101 (2016) 272–280.
[129] X. Guo, X. Li, Y. Xu, J. Chen, M. Lv, M. Yang, W. Chen, Understanding the Accelerated Sodium-Ion-Transport Mechanism of an Interfacial Modified Polyacrylonitrile Separator, J. Phys. Chem. C 126 (19) (2022) 8238–8247.
[130] X. Liu, K. Song, C. Lu, Y. Huang, X. Duan, S. Li, Y. Ding, Electrospun PU@GO separators for advanced lithium-ion batteries, J. Membr. Sci. 555 (2018) 1–6.
[131] K. Song, P. Zhang, Y. Huang, F. Xu, Y. Ding, Electrospun PU/PVP/GO Separator for Li-ion Batteries, Fibers Polym. 20 (5) (2019) 961–965.
[132] K. Song, Y. Huang, X. Liu, Y. Jiang, P. Zhang, Y. Ding, Electrospun PI@GO separators for Li-ion batteries: a possible solution for high-temperature operation, J. Sol-Gel Sci. Technol. 94 (1) (2020) 109–117.
[133] Q. Tian, Q. Liu, K. Song, Y. Mei, W. Lu, J. Peng, Y. Ding, Fabrication of Aligned PI/GO Nanofibers for Battery Separators, Fibers Polym. 22 (1) (2021) 30–35.
[134] X. Wang, H. Zhao, N. Deng, Y. Li, R. Yu, Y. Wen, B. Cheng, Efficient lithium-metal battery based on a graphene oxide-modified heat-resistant gel polymer electrolyte with superior cycling stability and excellent rate capability, Sustain. Energy Fuels 6 (2) (2022) 386–397.
[135] D. Kang, M. Xiao, J.P. Lemmon, Artificial Solid-Electrolyte Interphase for Lithium Metal Batteries, Batter Supercaps 4 (3) (2021) 445–455.
[136] L. Fan, M. Li, X. Li, W. Xiao, Z. Chen, J. Lu, Interlayer Material Selection for Lithium-Sulfur Batteries, Joule 3 (2) (2019) 361–386.
[137] J.-Q. Huang, Q. Zhang, F. Wei, Multi-functional separator/interlayer system for high-stable lithium-sulfur batteries: Progress and prospects, Energy Stor. Mater. 1 (2015) 127–145.
[138] S.H. Lee, J.R. Harding, D.S. Liu, J.M. D'Arcy, Y. Shao-Horn, P.T. Hammond, Li-Anode Protective Layers for Li Rechargeable Batteries via Layer-by-Layer Approaches, Chem. Mater. 26 (8) (2014) 2579–2585.
[139] J.-Q. Huang, Z.-L. Xu, S. Abouali, M. Akbari Garakani, J.-K. Kim, Porous Graphene Oxide/carbon Nanotube Hybrid Films as Interlayer for Lithium-Sulfur Batteries 99 (2016) 624–632.
[140] Y. Jiang, F. Chen, Y. Gao, Y. Wang, S. Wang, Q. Gao, Z. Chen, Inhibiting the shuttle effect of Li-S battery with a graphene oxide coating separator: Performance improvement and mechanism study, J. Power Sources 342 (2017) 929–938.
[141] W. Kong, L. Yan, Y. Luo, D. Wang, K. Jiang, Q. Li, J. Wang, Ultrathin MnO2/Graphene Oxide/Carbon Nanotube Interlayer as Efficient Polysulfide-Trapping Shield for High-Performance Li-S Batteries, Adv. Funct. Mater. 27 (18) (2017) n/a.
[142] Y.-D. Shen, Z.-C. Xiao, L.-X. Miao, D.-B. Kong, X.-Y. Zheng, Y.-H. Chang, L.-J. Zhi, Pyrolyzed bacterial cellulose/graphene oxide sandwich interlayer for lithium–sulfur batteries, Rare Met. 36 (5) (2017) 418–424.
[143] L. Yin, H. Dou, A. Wang, G. Xu, P. Nie, Z. Chang, X. Zhang, A functional interlayer as a polysulfides blocking layer for high-performance lithium-sulfur batteries, New J. Chem. 42 (2) (2018) 1431–1436.
[144] J.Y. Kim, D.O. Shin, K.M. Kim, J. Oh, J. Kim, S.H. Kang, Y.-G. Lee, Graphene Oxide Induced Surface Modification for Functional Separators in Lithium Secondary Batteries, Sci. Rep. 9 (1) (2019) 2464.
[145] X. Ni, T. Qian, X. Liu, N. Xu, J. Liu, C. Yan, High Lithium Ion Conductivity LiF/GO Solid Electrolyte Interphase Inhibiting the Shuttle of Lithium Polysulfides in Long-Life Li-S Batteries, Adv. Funct. Mater. 28 (13) (2018) n/a.
[146] D.K. Lee, S.J. Kim, Y.-J. Kim, H. Choi, D.W. Kim, H.-J. Jeon, H.-T. Jung, Graphene Oxide/Carbon Nanotube Bilayer Flexible Membrane for High-Performance Li-S Batteries with Superior Physical and Electrochemical Properties, Adv. Mater. Interfaces 6 (7) (2019) 1801992.
[147] M.S. Kiai, O. Eroglu, H. Kizil, Electrospun nanofiber polyacrylonitrile coated separators to suppress the shuttle effect for long-life lithium–sulfur battery, J. Appl. Polym. Sci. 137 (17) (2020) 48606.
[148] S. Ponnada, M.S. Kiai, D.B. Gorle, A. Nowduri, Application of Facile Graphene Oxide Binders with Nanocomposites for Efficient Separator Performance in Lithium Sulfur Batteries, Energy & Fuels 35 (15) (2021) 12619–12627.
[149] Q. Zeng, X. Leng, K.-H. Wu, I.R. Gentle, D.-W. Wang, Electroactive cellulose-supported graphene oxide interlayers for Li-S batteries, Carbon 93 (2015) 611–619.
[150] D. Liang, T. Bian, Q. Han, H. Wang, X. Song, B. Hu, Y. Zhao, Inhibiting the shuttle effect using artificial membranes with high lithium-ion content for enhancing the stability of the lithium anode, J. Mater. Chem. A 8 (28) (2020) 14062–14070.
[151] S.H. Park, T.H. Lee, Y.J. Lee, H.B. Park, Y.J. Lee, Graphene oxide sieving membrane for improved cycle life in high-efficiency redox-mediated Li-O2 batteries, Small 14 (34) (2018) n/a.
[152] H. Zhang, X. Ma, R. Chen, X. Wang, H. Ma, Y. Chai, M. Xue, Selective ion transport in assembled graphene oxide-modified separator and the novel intra-

series architecture for improved aqueous batteries, Chem. Eng. J. 450 (2022) 138061.
[153] M. Wang, Z. Peng, W. Luo, Q. Zhang, Z. Li, Y. Zhu, D. Wang, Improving the Interfacial Stability between Lithium and Solid-State Electrolyte via Dipole-Structured Lithium Layer Deposited on Graphene Oxide, *Adv. Sci. (Weinheim, Ger.)*, 7(13), (2020) 2000237.
[154] Y.-J. Zhang, X.-H. Xia, X.-L. Wang, C.-D. Gu, J.-P. Tu, Graphene oxide modified metallic lithium electrode and its electrochemical performances in lithium–sulfur full batteries and symmetric lithium–metal coin cells, RSC Adv. 6 (70) (2016) 66161–66168.
[155] G. Zhang, P. Li, K. Chen, H. Zheng, W. He, L. Xiao, J. Xu, A robust Janus bilayer with tailored ionic conductivity and interface stability for stable Li metal anodes, J. Energy Chem. 74 (2022) 368–375.
[156] Y. Gao, Z. Yan, J.L. Gray, X. He, D. Wang, T. Chen, D. Wang, Polymer-inorganic solid-electrolyte interphase for stable lithium metal batteries under lean electrolyte conditions, Nat. Mater. 18 (4) (2019) 384–389.
[157] Y. Wu, X. Sun, R. Li, C. Wang, D. Song, Z. Yang, J. Wu, In situ construction of trinity artificial protective layer between lithium metal and sulfide solid electrolyte interface, Electrochem. Commun. 142 (2022) 107377.
[158] Z.T. Wondimkun, T.T. Beyene, M.A. Weret, N.A. Sahalie, C.-J. Huang, B. Thirumalraj, B.-J. Hwang, Binder-free ultra-thin graphene oxide as an artificial solid electrolyte interphase for anode-free rechargeable lithium metal batteries, J. Power Sources 450 (2020) 227589.
[159] S.J.R. Prabakar, C. Park, A.B. Ikhe, K.-S. Sohn, M. Pyo, Simultaneous Suppression of Metal Corrosion and Electrolyte Decomposition by Graphene Oxide Protective Coating in Magnesium-Ion Batteries: Toward a 4-V-Wide Potential Window, ACS Appl. Mater. Interfaces 9 (50) (2017) 43767–43773.
[160] J. Xu, Z. Wei, P. Chen, W. Yan, T. Li, C. Chen, Enhancing the electrochemical behavior of Mg battery by using graphene conductive coating, Mater. Lett. 287 (2021) 129253.
[161] M. Shaibani, A. Akbari, P. Sheath, C.D. Easton, P.C. Banerjee, K. Konstas, M. Majumder, Suppressed Polysulfide Crossover in Li-S Batteries through a High-Flux Graphene Oxide Membrane Supported on a Sulfur Cathode, ACS Nano 10 (8) (2016) 7768–7779.
[162] S. Nam, J. Kim, V.H. Nguyen, M. Mahato, S. Oh, P. Thangasamy, I.-K. Oh, Collectively Exhaustive MXene and Graphene Oxide Multilayer for Suppressing Shuttling Effect in Flexible Lithium Sulfur Battery, Adv. Mater. Technol. 7 (5) (2022) 2101025.
[163] C. Wu, W. Zeng, Gel Electrolyte for Li Metal Battery, Chem. Asian J. 17 (23) (2022) e202200816.
[164] J. Pan, N. Wang, H.J. Fan, Gel Polymer Electrolytes Design for Na-Ion Batteries, Small Methods 6 (11) (2022) 2201032.
[165] X. Yang, F. Zhang, L. Zhang, T. Zhang, Y. Huang, Y. Chen, A High-Performance Graphene Oxide-Doped Ion Gel as Gel Polymer Electrolyte for All-Solid-State Supercapacitor Applications, Adv. Funct. Mater. 23 (26) (2013) 3353–3360.
[166] X. Yang, L. Zhang, F. Zhang, T. Zhang, Y. Huang, Y. Chen, A high-performance all-solid-state supercapacitor with graphene-doped carbon material electrodes and a graphene oxide-doped ion gel electrolyte, Carbon 72 (2014) 381–386.
[167] X. Zhao, C.-A. Tao, Y. Li, X. Chen, J. Wang, H. Gong, Preparation of gel polymer electrolyte with high lithium ion transference number using GO as filler and application in lithium battery, Ionics 26 (9) (2020) 4299–4309.
[168] X. Zhao, Z. Wu, Z. Zhang, N. Wang, C.-A. Tao, J. Wang, H. Gong, The polymer composite electrolyte with polyethylene oxide-grafted graphene oxide as fillers toward stable highcurrent density lithium metal anodes, Mater. Res. Express 8 (10) (2021) 105305.
[169] W. Shen, K. Li, Y. Lv, T. Xu, D. Wei, Z. Liu, Highly-Safe and Ultra-Stable All-Flexible Gel Polymer Lithium Ion Batteries Aiming for Scalable Applications, Adv. Energy Mater. 10 (21) (2020) 1904281.
[170] K. Li, W. Shen, T. Xu, L. Yang, X. Xu, F. Yang, D. Wei, Fibrous gel polymer electrolyte for an ultrastable and highly safe flexible lithium-ion battery in a wide temperature range, Carbon Energy 3 (6) (2021) 916–928.
[171] M. Hamrahjoo, S. Hadad, E. Dehghani, M. Salami-Kalajahi, H. Roghani-Mamaqani, Poly(poly[ethylene glycol] methyl ether methacrylate)/graphene oxide nanocomposite gel polymer electrolytes prepared by controlled and conventional radical polymerizations for lithium ion batteries, Int. J. Energy Res. 46 (7) (2022) 9114–9127.
[172] T. Yang, C. Shu, Z. Hou, R. Zheng, H. Peng, M. Li, J. Long, 3D porous network gel polymer electrolyte with high transference number for dendrite-free Li-O2 batteries, Solid State Ion 343 (2019) 115088.
[173] Z. Song, J. Ding, B. Liu, X. Liu, X. Han, Y. Deng, C. Zhong, A Rechargeable Zn–Air Battery with High Energy Efficiency and Long Life Enabled by a Highly Water-Retentive Gel Electrolyte with Reaction Modifier, Adv. Mater. 32 (22) (2020) 1908127.
[174] W.-C. Lai, R.-W. Fan, A simple low-cost method to prepare gel electrolytes incorporating graphene oxide with increased ionic conductivity and electrochemical stability, J. Electroanal. Chem. 907 (2022) 115889.
[175] L. Lv, B. Hui, X. Zhang, Y. Zou, D. Yang, Lamellar agarose/graphene oxide gel polymer electrolyte network for all-solid-state supercapacitor, Chem. Eng. J. 452 (2023) 139443.
[176] F. He, Z. Hu, W. Tang, A. Wang, B. Wen, L. Zhang, J. Luo, Vertically Heterostructured Solid Electrolytes for Lithium Metal Batteries, Adv. Funct. Mater. 32 (25) (2022) 2201465.
[177] Z. Xue, D. He, X. Xie, Poly(ethylene oxide)-based electrolytes for lithium-ion batteries, J. Mater. Chem. A 3 (38) (2015) 19218–19253.
[178] D.E. Fenton, J.M. Parker, P.V. Wright, Complexes of alkali metal ions with poly (ethylene oxide), Polymer 14 (11) (1973) 589.
[179] C. Berthier, W. Gorecki, M. Minier, M.B. Armand, J.M. Chabagno, P. Rigaud, Microscopic investigation of ionic conductivity in alkali metal salts-poly(ethylene oxide) adducts, Solid State Ion 11 (1) (1983) 91–95.
[180] Y.-C. Cao, C. Xu, X. Wu, X. Wang, L. Xing, K. Scott, A poly (ethylene oxide)/graphene oxide electrolyte membrane for low temperature polymer fuel cells, J. Power Sources 196 (20) (2011) 8377–8382.
[181] M. Yuan, J. Erdman, C. Tang, H. Ardebili, High performance solid polymer electrolyte with graphene oxide nanosheets, RSC Adv. 4 (103) (2014) 59637–59642.
[182] S. Gao, J. Zhong, G. Xue, B. Wang, Ion conductivity improved polyethylene oxide/lithium perchlorate electrolyte membranes modified by graphene oxide, J. Membr. Sci. 470 (2014) 316–322.
[183] M.S. Khan, A. Shakoor, Ionic Conductance, Thermal and Morphological Behavior of PEO-Graphene Oxide-Salts Composites, J. Chem. 2015 (2015) 695930.
[184] M. Kammoun, S. Berg, H. Ardebili, Flexible thin-film battery based on graphene-oxide embedded in solid polymer electrolyte, Nanoscale 7 (41) (2015) 17516–17522.
[185] S. Cheng, D.M. Smith, C.Y. Li, How Does Nanoscale Crystalline Structure Affect Ion Transport in Solid Polymer Electrolytes? Macromolecules 47 (12) (2014) 3978–3986.
[186] J. Mohanta, D.K. Padhi, S. Si, Li-ion conductivity in PEO-graphene oxide nanocomposite polymer electrolytes: A study on effect of the counter anion, J. Appl. Polym. Sci. 135 (22) (2018) n/a.
[187] J. Wen, Q. Zhao, X. Jiang, G. Ji, R. Wang, G. Lu, C. Xu, Graphene Oxide Enabled Flexible PEO-Based Solid Polymer Electrolyte for All-Solid-State Lithium Metal Battery, ACS Appl. Energy Mater. 4 (4) (2021) 3660–3669.
[188] L. Zhang, G. Jin, T. Ma, S. Wang, Ion transport in topological all-solid-state polymer electrolyte improved via graphene-oxide, J. Appl. Polym. Sci. 138 (14) (2021) 50173.
[189] H.K. Koduru, M.T. Iliev, K.K. Kondamareddy, D. Karashanova, T. Vlakhov, X. Z. Zhao, N. Scaramuzz, Investigations on Poly (ethylene oxide) (PEO) - blend based solid polymer electrolytes for sodium ion batteries, J. Phys.: Conf. Ser. 764 (2016) 012006/012001.
[190] H.K. Koduru, F. Scarpelli, Y.G. Marinov, G.B. Hadjichristov, P.M. Rafailov, I. K. Miloushev, N. Scaramuzza, Characterization of PEO/PVP/GO nanocomposite solid polymer electrolyte membranes: microstructural, thermo-mechanical, and conductivity properties, Ionics 24 (11) (2018) 3459–3473.
[191] T.E. Vlakhov, Y.G. Marinov, G.B. Hadjichristov, N. Scaramuzza, Complex electrical impedance and dielectric spectroscopy of Na+-conducting PEO/PVP/NaIO4 solid polymer electrolyte with incorporated nano-sized Graphene Oxide, J. Phys.: Conf. Ser. 1762 (2021) 012010.
[192] H.K. Koduru, L. Bruno, Y.G. Marinov, G.B. Hadjichristov, N. Scaramuzza, Mechanical and sodium ion conductivity properties of graphene oxide-incorporated nanocomposite polymer electrolyte membranes, J. Solid State Electrochem. 23 (9) (2019) 2707–2722.
[193] X. Zhou, P. Lv, M. Li, J. Xu, G. Cheng, N. Yuan, J. Ding, Graphene Oxide Aerogel Foam Constructed All-Solid Electrolyte Membranes for Lithium Batteries, Langmuir 38 (10) (2022) 3257–3264.
[194] S. Gomari, M. Esfandeh, I. Ghasemi, All-solid-state flexible nanocomposite polymer electrolytes based on poly(ethylene oxide): Lithium perchlorate using functionalized graphene, Solid State Ion 303 (2017) 37–46.
[195] Z. Hu, X. Zhang, S. Chen, A graphene oxide and ionic liquid assisted anion-immobilized polymer electrolyte with high ionic conductivity for dendrite-free lithium metal batteries, J. Power Sources 477 (2020) 228754.
[196] J. Li, Y. Cai, H. Wu, Z. Yu, X. Yan, Q. Zhang, Z. Bao, Polymers in Lithium-Ion and Lithium Metal Batteries, Adv Energy Mater 11 (15) (2021) 2003239.
[197] H. Bashirpour-Bonab, Analysis of the effect of graphene oxide on polymer electrolytes based on PVDF for lithium-ion battery, Int. J. Energy Res. 46 (11) (2022) 15793–15803.
[198] A.L. Ahmad, U.R. Farooqui, N.A. Hamid, Effect of graphene oxide (GO) on Poly (vinylidene fluoride-hexafluoropropylene) (PVDF-HFP) polymer electrolyte membrane, Polymer 142 (2018) 330–336.
[199] S. Majumdar, P. Sen, R. Ray, Graphene oxide induced high dielectricity in CS/PMMA solid polymer electrolytes and the enhanced specific capacitance with Ag decorated MnCoFeO4 nanoparticles anchored graphene sheets in hybrid solid-state supercapacitors, Mater. Res. Bull. 151 (2022) 111814.
[200] Y.D. Lee, J. Yuenyongsuwan, P. Nanthananon, Y.K. Kwon, Polyimide hybrid membranes with graphene oxide for lithium-sulfur battery separator applications, Polymer 255 (2022) 125110.
[201] M.M. Hassan, A.A. Bristi, X. He, M. Trifkovic, G. Bobrov, Q. Lu, Novel nanoarchitecture of 3D ion transfer channel containing nanocomposite solid polymer electrolyte membrane based on holey graphene oxide and chitosan biopolymer, Chem. Eng. J. 466 (2023) 143159.
[202] M. Fouladvand, L. Naji, M. Javanbakht, A. Rahmanian, Electrochemical characterization of Li-ion conducting polyvinylidene fluoride/sulfonated graphene oxide nanocomposite polymer electrolyte membranes for lithium ion batteries, J. Membr. Sci. 636 (2021) 119563.
[203] J. Li, Y. Li, J. Cheng, Q. Sun, L. Dai, X. Nie, L. Ci, A graphene oxide coated sulfide-based solid electrolyte for dendrite-free lithium metal batteries, Carbon 177 (2021) 52–59.
[204] K.J. Lee, Y.H. Chu, Preparation of the graphene oxide (GO)/Nafion composite membrane for the vanadium redox flow battery (VRB) system, Vacuum 107 (2014) 269–276.
[205] Y.G. Shul, Y.H. Chu, Nafion/Graphene Oxide Layered Structure Membrane for the Vanadium Redox Flow Battery, Sci. Adv. Mater. 6 (7) (2014) 1445–1452.

[206] L. Yu, F. Lin, L. Xu, J. Xi, A recast Nafion/graphene oxide composite membrane for advanced vanadium redox flow batteries, RSC Adv. 6 (5) (2016) 3756–3763.
[207] L. Su, D. Zhang, S. Peng, X. Wu, Y. Luo, G. He, Orientated graphene oxide/Nafion ultra-thin layer coated composite membranes for vanadium redox flow battery, Int. J. Hydrogen Eenergy 42 (34) (2017) 21806–21816.
[208] W. Dai, Y. Shen, Z. Li, L. Yu, J. Xi, X. Qiu, SPEEK/Graphene oxide nanocomposite membranes with superior cyclability for highly efficient vanadium redox flow battery, J. Mater. Chem. A 2 (31) (2014) 12423–12432.
[209] C. Wu, H. Bai, Y. Lv, Z. Lv, Y. Xiang, S. Lu, Enhanced membrane ion selectivity by incorporating graphene oxide nanosheet for vanadium redox flow battery application, Electrochim. Acta 248 (2017) 454–461.
[210] W. Dai, L. Yu, Z. Li, J. Yan, L. Liu, J. Xi, X. Qiu, Sulfonated Poly(Ether Ether Ketone)/Graphene composite membrane for vanadium redox flow battery, Electrochim. Acta 132 (2014) 200–207.
[211] S. Yuan, K. Ding, X. Zeng, D. Bin, Y. Zhang, P. Dong, Y. Wang, Advanced Non-Flammable Organic Electrolyte Promises Safer Li Metal Batteries: From Solvation Structure Perspectives, *Adv. Mater.*, n/a(n/a), 2206228.
[212] H. Wang, Z. Yu, X. Kong, S.C. Kim, D.T. Boyle, J. Qin, Y. Cui, Liquid electrolyte: The nexus of practical lithium metal batteries, Joule 6 (3) (2022) 588–616.
[213] Y. Yu, Y. Liu, J. Xie, Building Better Li Metal Anodes in Liquid Electrolyte: Challenges and Progress, ACS Appl. Mater. Interfaces 13 (1) (2021) 18–33.
[214] X. Wang, A.V. Kirianova, X. Xu, Y. Liu, O.O. Kapitanova, M.O. Gallyamov, Novel electrolyte additive of graphene oxide for prolonging the lifespan of zinc-ion batteries, Nanotechnology 33 (12) (2021).